

In-Depth Study of Tripeptide-Based α -Ketoheterocycles as Inhibitors of Thrombin. Effective Utilization of the S₁' Subsite and Its Implications to Structure-Based Drug Design¹

Michael J. Costanzo,* Harold R. Almond, Jr., Leonard R. Hecker, Mary R. Schott, Stephen C. Yabut, Han-Cheng Zhang, Patricia Andrade-Gordon, Thomas W. Corcoran, Edward C. Giardino, Jack A. Kauffman, Joan M. Lewis, Lawrence de Garavilla, Barbara J. Haertlein, and Bruce E. Maryanoff*

Drug Discovery, Johnson & Johnson Pharmaceutical Research & Development,[†] Spring House, Pennsylvania 19477-0776

Received August 14, 2003

Thrombin inhibitors are potentially useful in medicine for their anticoagulant and antithrombotic effects. We synthesized and evaluated diverse heterocycle-activated ketones based on the D-Phe-Pro-Arg, and related thrombin active-site recognition motifs, as candidate inhibitors. The peptide-based α -ketoheterocycles were typically prepared by either an imidate or a Weinreb amide route (Schemes 1 and 2), the latter of which proved to be more general. Test compounds were generally assayed for inhibition of human α -thrombin and bovine trypsin. From a structure-based design standpoint, the heterocycle allows one to explore and adjust interactions within the S₁' subsite of thrombin. The preferred α -ketoheterocycle is a π -rich 2-substituted azole with at least two heteroatoms proximal to the carbon bearing the keto group, and a preferred thrombin inhibitor is 2-ketobenzothiazole **3**, with a potent K_i value of 0.2 nM and ca. 15-fold selectivity over trypsin. 2-Ketobenzothiazole **13** exhibited exceedingly potent thrombin inhibition ($K_i = 0.00065$ nM; slow tight binding). Several α -ketoheterocycles had thrombin K_i values in the range 0.1–400 nM. The "Arg" unit in the α -ketoheterocycles can be sensitive to stereomutation under mildly basic conditions. For example, 2-ketothiazoles **4** and **59** readily epimerize at pH 7.4, although they are fairly stable stereochemically at pH 3–4; thus, suitable conditions had to be selected for the enzymatic assays. Lead D-Phe-Pro-Arg 2-benzothiazoles **3**, **4**, and **68** displayed good selectivity for thrombin over other key coagulation enzymes (e.g., factor Xa, plasmin, protein C, uPA, tPA, and streptokinase); however, their selectivity for thrombin over trypsin was modest (<25-fold). Compounds **3**, **4**, and **68** exhibited potent *in vitro* antithrombotic activity as measured by inhibition of gel-filtered platelet aggregation induced by α -thrombin ($IC_{50} = 30$ – 40 nM). They also proved to be potent anticoagulant/antithrombotic agents *in vivo* on intravenous administration, as determined in the canine arteriovenous shunt ($ED_{50} = 0.45$ – 0.65 mg/kg) and the rabbit deep vein thrombosis ($ED_{50} = 0.1$ – 0.4 mg/kg) models. Intravenous administration of **3**, and several analogues, to guinea pigs caused hypotension and electrocardiogram abnormalities. Such cardiovascular side effects were also observed with some nonguanidine inhibitors and inhibitors having recognition motifs other than D-Phe-Pro-Arg. 2-Benzothiazolecarboxylates **4** and **68** exhibited significantly diminished cardiovascular side effects, and benzothiazolecarboxylic acid **4** had the best profile with respect to therapeutic index. The X-ray crystal structures of the ternary complexes **3**–thrombin–hirugen and **4**–thrombin–hirugen depict novel interactions in the S₁' region, with the benzothiazole ring forming a hydrogen bond with His-57 and an aromatic stacking interaction with Trp-60D of thrombin's insertion loop. The benzothiazole ring of **3** displaces the Lys-60F side chain into a U-shaped gauche conformation, whereas the benzothiazole carboxylate of **4** forms a salt bridge with the side chain of Lys-60F such that it adopts an extended anti conformation. Since **3** has a 10-fold greater affinity for thrombin than does **4**, any increase in binding energy resulting from this salt bridge is apparently offset by perturbations across the enzyme (*viz.* Figure 4). The increased affinity and selectivity of 2-ketobenzothiazole inhibitors, such as **3**, may be primarily due to the aromatic stacking interaction with Trp-60D. However, energy contour calculations with the computer program GRID also indicate a favorable interaction between the benzothiazole sulfur atom and a hydrophobic patch on the surface of thrombin.

The analysis of macromolecular structures by X-ray crystallography, NMR studies, and computer-assisted molecular modeling can provide well-defined, three-

dimensional structures for use in drug design and optimization.² Structure-based drug design has been especially well suited for agents that inactivate enzyme targets. In this regard, particular attention has been directed to the serine protease α -thrombin (EC 3.4.21.5)³ following the first X-ray structure, which was reported in 1989.⁴ Since thrombin has a critical position in the

* Address correspondence to these authors. For M.J.C.: phone, 215-628-5648; fax, 215-628-4985; e-mail, mcostanz@prdus.jnj.com. For B.E.M.: phone, 215-628-5530; fax, 215-628-4985; e-mail, bmaryano@prdus.jnj.com.

[†] Formerly The R. W. Johnson Pharmaceutical Research Institute.

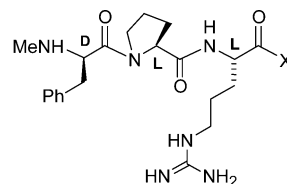
blood coagulation cascade and thus a central role in the regulation of hemostasis and thrombosis,⁵ inhibitors of this enzyme could lead to useful drugs for treating thrombotic disorders,⁶ which constitute a serious source of mortality and morbidity in patients worldwide.

Bode et al.⁴ described the molecular structure of human α -thrombin complexed with D-Phe-Pro-Arg-CH₂-Cl (**1a**, PPACK),⁷ an irreversible active-site inhibitor (a "transition-state analogue").⁸ This archetypal complex reveals numerous key interactions at the atomic level: (1) an antiparallel β -strand between the extended backbone of the ligand and the backbone of Ser-214/Trp-215/Gly-216; (2) the guanidine occupying the S₁ specificity pocket; (3) a tetrahedral adduct formed with Ser-195; (4) alkylation of the ϵ -nitrogen of His-57 via the chloromethyl group; (5) the methylene groups of Pro tucked into a hydrophobic S₂ cleft partly defined by residues of the 60A-I insertion loop; and (6) the phenyl group of D-Phe in a hydrophobic S₃ pocket with an aromatic stacking interaction involving Trp-215.⁹ Additionally, the X-ray crystal structure of thrombin-PPACK (viz. **1a**) suggests an opportunity for specific interactions with the unique 60A-I insertion loop of thrombin, especially with the side chains of Tyr-60A, Trp-60D, and Lys-60F. Shortly thereafter, Tulinsky, Bode, and co-workers¹⁰ determined the molecular structure of human α -thrombin complexed with r-hirudin, a des-sulfate version of the famous anticoagulant protein from the European medicinal leech, which depicts an elaborate collection of hydrogen bonds and electrostatic interactions. These achievements set the stage for thrombin to become a preeminent target for structure-based drug design.

In 1991, we developed an interest in thrombin as a therapeutic target and embarked on a project to discover novel inhibitors with the aid of published atomic coordinates and computer-based molecular modeling. One of our approaches involved the synthesis and biological evaluation of peptide-based α -ketoheterocycles (also termed "acylheterocycles"), adapted from the proven thrombin recognition motif D-Phe-Pro-Arg-X, which is exemplified by the chloromethyl ketone PPACK (**1a**)⁷ and the aldehyde efegatran (**1b**).¹¹ Such tripeptide species tend to operate as "transition-state analogues" in the region of the thrombin catalytic triad, the focal point of substrate proteolytic cleavage.⁸ We envisioned the substitution of "X" with heterocycles such as 2-oxazolyl or 2-pyridyl to obtain "heterocycle-activated ketones" that would form a reversible hemiketal adduct with the γ -oxygen of Ser-195, a key residue of the active-site catalytic triad. This strategy seemed particularly attractive because heterocycles, besides furnishing the necessary electrophilicity to the arginine carbonyl, could serve as a "C-terminal extensor" into the S₁' region of the thrombin active site to probe for additional useful interactions. This group, along with its substituents, would allow for modulation of electronic and steric properties to adjust the interactions.

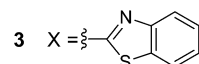
Concurrently, we had been investigating the sponge-derived natural product cyclotheonamide A (**2**, CtA),¹² a macrocyclic thrombin inhibitor, as well as its congeners.¹³ CtA intrigued us in several ways, but it was most useful as a tool for elucidating new types of interactions within the active site of thrombin. Therefore, we deter-

mined the molecular structure of the CtA-thrombin-hirugen complex.^{12a} In addition to the expected features of CtA complexation relative to its Pro-Arg motif and its electrophilic α -ketoamide, we also found an aromatic stacking interaction within the S₁' region of the active site between the hydroxyphenyl group of CtA and Trp-60D. This observation supported the idea of finding new worthwhile interactions in the S₁' domain of thrombin, and we pursued this avenue by means of peptide-based α -ketoheterocycles. This "heterocycle-activated ketone" approach was quite successful, as documented in our preliminary publication on a series of potent thrombin inhibitors.¹⁴ Subsequently, we presented details on the X-ray crystal structures of thrombin complexed with our inhibitors RWJ-50353 (**3**)^{15a} and RWJ-51438 (**4**),^{15b} as well as on the antithrombotic properties of **3**.¹⁶

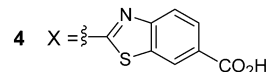


1a X = CH₂Cl (PPACK)

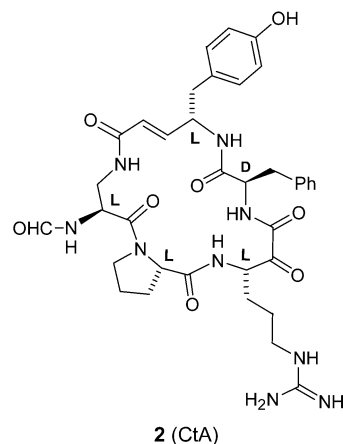
1b X = H (efegatran)



3 X =

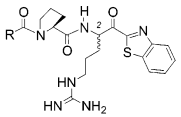


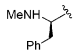
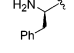
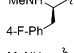
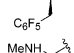
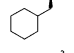
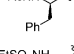
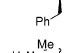
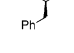
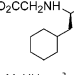
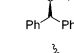
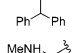
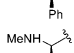
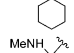
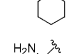
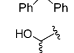
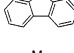
4 X =



2 (CtA)

During the early phase of our studies, Edwards et al. published pioneering work on peptide-based α -ketoheterocycles as serine protease inhibitors, in their case for elastase.¹⁷ A seminal paper in 1992 described the first examples of such compounds and presented an X-ray crystal structure of Ac-Val-Pro-Val-(2-benzoxazole) complexed with porcine pancreatic elastase (PPE).^{17a} This structure revealed the key features of hemiketal formation with Ser-195 and hydrogen bonding between the benzoxazole nitrogen and His-57.^{17a} Such interactions were subsequently identified in our work on peptide-based α -ketoheterocycles and thrombin.^{14,15} Over the ensuing years, there have been many other papers dealing with peptide-based α -ketoheterocycles as inhibitors of thrombin,¹⁸ various serine proteases,¹⁹ and cysteine proteases.²⁰ While this structural motif has

Table 1. Biological Data for P3 Analogues


compd ^a	R	2S/2R ^b	thr K _i , nM ^c	thr IC ₅₀ , nM ^c	try K _i , nM ^c
3		49:1	0.20 ± 0.02 (30)	29 ± 11 (3)	3.1 ± 0.7 (9) ^d
5 ^e		15.7:1	SB ^f	21 ± 16 (2)	0.3 ± 0.1 (3)
6		32:1 ^g	0.12 ± 0.01 (6)	15 ± 12 (2)	3.3 ± 1.5 (3)
7		49:1	3.8 ± 0.3 (6)	150 ± 40 (5)	9.3 ± 6.7 (7)
8		32:1	0.18 ± 0.03 (4)	48 ± 20 (3)	3.9 ± 2.4 (2)
9		2.8:1 ^g	13 ± 1 (6)	430 ± 100 (4)	2.4 ± 0.7 (4)
10		5.7:1	24 ± 4 (3)	500 (1)	31 ± 5 (3)
11		ND	0.20 ± 0.04 (6)	3.5 ± 0.5 (2)	3.9 ± 1.3(6)
12		5.3:1	0.36 ± 0.09 (4)	29 ± 13 (3)	22 ± 7 (3)
13		99:1	SB ^h	4.5 ± 3.5 (2)	ND ⁱ
14		3:1	1.1 ± 0.3 (6)	11 (1)	22 ± 8 (8)
15		5.8:1 ^j	0.46 ± 0.05 (6)	34 ± 7 (5)	ND ^k
16		99:1	SB ^l	5.3 ± 0.4 (49)	1.2 ± 0.6 (3)
17		32:1	73 ± 22 (6)	490 ± 120 (2)	2.6 ± 0.4 (6)
18		ND	2.1 ± 0.7 (6)	15 (1)	1.8 ± 0.6 (5)
19		1.4:1	3.1 ± 0.1 (3)	95 ± 22 (7)	2.0 (1)
20	Me	1.0:1	ND	14000 ± 400 (7)	3.7 ± 0.7 (4)

^a Trifluoroacetate salt. ^b The 2S/2R epimeric ratio was determined by analytical HPLC except where otherwise noted. ^c Abbreviations: thr, human α -thrombin; try, bovine trypsin; ND, not determined; SB, slow-binding kinetics. Standard errors are given for *N* experiments, which are indicated in parentheses. ^d IC₅₀ = 30 ± 5 nM (*N* = 5). ^e The L-Phe diastereomer of **5** (**78**; 2S/2R = 99:1) had thrombin and trypsin IC₅₀ values of 17000 ± 1300 nM and 5.8 ± 0.6 nM (*N* = 2), respectively. ^f Slow-binding K_i = 0.0055 ± 0.0043 nM (*N* = 2). ^g Determined by ¹H NMR via the ratio of the α -methine peak integrals. ^h Slow-binding K_i = 0.00065 ± 0.00009 nM (*N* = 2). ⁱ IC₅₀ = 30 ± 7 nM (*N* = 4). ^j Determined by ¹H NMR via the ratio of the *N*-methyl peak integrals. ^k IC₅₀ = 32 ± 14 nM (*N* = 4). ^l Slow-binding K_i = 0.018 ± 0.011 nM (*N* = 2).

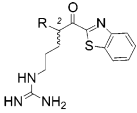
generally afforded very potent enzyme inhibitors, the verdict is still out as to whether such “transition-state analogues” can also provide viable drug candidates for clinical development.

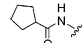
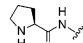
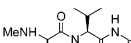
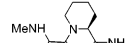
In this article, we present a detailed report on our studies with peptide-based α -ketoheterocycles as inhibitors of thrombin. This effort has encompassed a diverse set of molecular entities, which are represented by structures **3–77**. Overall, we address (1) the design and synthesis of potent, selective thrombin inhibitors, generally based on D-Phe-Pro-Arg and related motifs; (2) the epimerization potential at the stereogenic center α to the heterocycle-activated ketone; (3) structure–activity relationships (SAR); (4) the efficacy of selected

inhibitors in animal models of thrombosis; (5) structural changes to circumvent problematic side effects; and (6) noteworthy aspects of intermolecular interactions within the active site of thrombin from X-ray structures of complexes.

Results and Discussion

Initially, we set out to investigate tripeptide-based α -ketoheterocycles based on the D-Phe-Pro-Arg sequence (**3–68**) (Tables 1–5), a proven thrombin recognition motif. Later, we attached the favored α -keto-2-benzothiazole to other known thrombin recognition motifs (**69–77**) (Table 6). An N-terminal *N*-methyl group was installed in most of the D-Phe-Pro-Arg compounds and

Table 2. Biological Data for P₂ Analogues


compd ^a	R	2S/2R ^b	thr K _i , nM ^c	thr IC ₅₀ , nM ^c	try K _i , nM ^c
21 ^d	H	---	ND	NA @ 300 μ M	NA @ 100 μ M
22	HC(O)NH-	ND	ND	>50000 (1)	1300 \pm 300 (6)
23 ^d		1.7:1 ^e	14600 \pm 100 (3)	82000 \pm 29000 (2)	30 \pm 6 (6)
24		ND	ND	>100000 (1)	250 \pm 30 (6)
25		2.3:1	21 \pm 7 (6)	440 \pm 170 (4)	1.5 \pm 0.5 (6)
26		4.8:1 ^f	0.34 \pm 0.5 (6)	38 \pm 13 (4)	1.8 \pm 0.4 (4)

^a Trifluoroacetate salt. ^b The 2S/2R epimeric ratio was determined by analytical HPLC except where otherwise noted. ^c Abbreviations: thr, human α -thrombin; try, bovine trypsin; NA, not active (less than 10% inhibition at the specified concentration); ND, not determined. Standard errors are given for *N* experiments (indicated in parentheses). ^d Compound reported in ref 19j. ^e Determined by ¹³C NMR via the integrals for the peaks at δ 122.32 and 122.16 ppm in the presence of 4.3 mol equiv of (*R*)-(-)-2,2,2-trifluoro-1-(9-anthryl)ethanol in CDCl₃ at 40 °C. ^f Determined by ¹H NMR via integration of the *N*-methyl peaks.

congeners to avoid possible imine formation between a primary amino N-terminus and the activated ketone, which could lead to self-condensation or decomposition. Whereas the tripeptide aldehyde D-Phe-Pro-Arg-H (GYKI-14166) self-condenses to an imidazo[1,2-*a*]pyrrolo[2,1-*c*]pyrazine system,^{11a} the corresponding *N*-methyl analogue (**1b**, efegatran) is not plagued by this problem.¹¹ We prepared numerous tripeptide α -ketoheterocycles with 2-substituted π -rich heterocycles (**3–49**, **51–55**, **57–77**), as well as two with 2-substituted π -deficient heterocycles (**50** and **56**) (Tables 1–6). Our emphasis on the π -rich heterocycles was derived from the fact that they generally exhibited much better potency as thrombin inhibitors (vide infra).

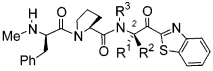
Synthetic Chemistry. Target compounds **3–77** were synthesized by two main routes, which are illustrated for the synthesis of **3** and **4** in Schemes 1 and 2, respectively.²¹ In the first route, the heterocycle was formed by reacting a hydroxyimide, such as **3b**, with an appropriate bifunctional amine (Scheme 1). The hydroxyimides were prepared by reacting either a tripeptidyl aldehyde, such as **3a**,^{11a} or a protected amino acid aldehyde with acetone cyanohydrin^{17a} and treating the resulting adduct with methanolic HCl. As an example, reaction of **3b** with 2-aminothiophenol furnished benzothiazole **3c**, which was oxidized with the Dess–Martin periodinane,²³ deprotected with HF, and purified by HPLC to furnish benzothiazole **3**.

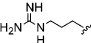
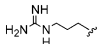
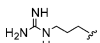
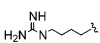
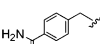
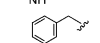
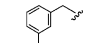
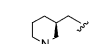
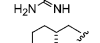
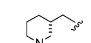
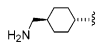
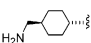
In the second route, the heterocycle was introduced by reacting a Weinreb amide, such as **4a**,²⁴ with an appropriate lithioheterocycle at low temperature (Scheme 2). Excess lithium reagent was required to overcome quenching caused by the exchangeable protons in the substrate. We preferred arylsulfonyl protecting groups for the Arg guanidine because benzyloxycarbonyl (Cbz) and 9-fluorenylmethylcarbonyl (Fmoc) groups were cleaved too readily under the reaction conditions. Hence, treatment of Weinreb amide **4a** with 5–8 mol equiv of lithium 2-lithiobenzothiazole-6-carboxylate at -78 °C provided the corresponding ketone, which was reduced

with NaBH₄²⁵ (to avoid side reactions during the ensuing steps), esterified with trimethylsilyldiazomethane, and deprotected with trifluoroacetic acid (TFA) to yield alcohols **4b**. Dipeptide **4c** was coupled to **4b** with the agency of dicyclohexylcarbodiimide (DCC) to give intermediate **4d**, which was saponified and converted to benzothiazolecarboxylic acid **4** by the methods used for **3c** (Scheme 1). In the synthesis of lysine-based and analogous target compounds (**37–42**, **69–72**), the amino side chain was protected with a 4-methoxy-2,3,6-trimethylbenzenesulfonyl (Mtr) group, which was removed by using anhydrous HBr in the final deprotection step. The diastereomeric alcohols corresponding to **3**, **48**, and **49**, were prepared by HF deprotection of **3c** followed by HPLC separation. The second route (Scheme 2) is more convergent and proved to be more versatile.

The crude target compounds from both routes usually contained 10–20% of the epimeric D-amino ketone diastereomer (e.g., **27**, **33**, **36**, **38**, **40**, and **42**),²⁶ most of which was removed during purification by reverse-phase HPLC. The D-amino ketone diastereomer, which generally eluted before the corresponding L-diastereomer, had greatly diminished thrombin and trypsin affinities relative to the L-diastereomer (vide infra). The L/D-amino ketone diastereomer ratios (2S/2R) were usually determined by either analytical HPLC or proton NMR integration of the *N*-methyl or amino ketone α -methine signals.

Compounds **28**, **41/42**, **43**, **71/72** required the synthesis of various unnatural amino acids (Schemes 3–6). α -L-Methylarginine derivative **28** was prepared by the route illustrated in Scheme 3. Orthogonal protection of α -L-ornithine²⁷ (**28a**) with Cbz and *tert*-butyloxycarbonyl (Boc) groups gave **28b**, which was guanylated to provide protected Arg derivative **28c**. After removal of the two Cbz groups from **28c**, tosylation and esterification furnished ester **28d**. Reaction of **28d** with 2-lithiobenzothiazole, followed by reduction of the ketone moiety and removal of the Boc group, furnished **28e**, which was

Table 3. Biological Data for P₁ Analogues


cmpd ^a	R ¹	R ²	R ³	2S/2R ^b	thr K _i , nM ^c	thr IC ₅₀ , nM ^c	try K _i , nM ^c
27	H		H	1:99	17 ± 6 (3)	80 (1)	26 ± 8 (7)
28		Me	H	14:1 ^d	SB ^e	3700 ± 2800 (2)	6000 ± 1400 (5)
29		H	Me	99:1 ^d	2100 ± 300 (6)	21000 (1)	5300 ± 1000 (5)
30		H	H	32:1	ND	8400 (1)	ND ^f
31		H	H	4:1	1400 ± 200 (6)	NA @ 1 μM	ND ^g
32		H	H	49:1	0.99 ± 0.06 (3)	ND	1.8 ± 1.0 (3)
33	H		H	1:99	15 ± 5 (2)	370 ± 290 (2)	2600 ± 2200 (4)
34		H	H	99:1	1.6 ± 0.1 (3)	51 ± 20 (3)	8.0 ± 1.0 (3)
35		H	H	99:1	99 ± 7 (3)	1000 (1)	210 ± 20 (3)
36	H		H	1:99	380 ± 90 (3)	ND	540 ± 350 (3)
37	H ₂ N(CH ₂) ₄ - ξ	H	H	99:1 ^d	38 ± 5(3)	650 ± 240 (2)	4.3 ± 1.5 (3)
38	H	H ₂ N(CH ₂) ₄ - ξ	H	1:99 ^d	210 ± 10 (3)	ND	20 ± 11 (3)
39	MeNH(CH ₂) ₄ - ξ	H	H	9:1 ^h	3700 ± 600 (3)	NA @ 1 μM	1200 ± 800 (3)
40	H	MeNH(CH ₂) ₄ - ξ	H	1:12 ^h	3500 ± 1300 (6)	NA @ 1 μM	1000 ± 400 (3)
41		H	H	99:1	920 (1)	17000 ± 14000 (2)	54 ± 0 (2)
42	H		H	1:99	1450 (1)	NA @ 1 μM	4000 (1)
43	MeO(CH ₂) ₃ - ξ	H	H	4:1 ^h	3900 ± 1000 (6)	46000 (1)	12000 ± 1000 (3)
44	Bu	H	H	10:1	ND	>100000	NA @ 1 μM
45	Bzl	H	H	5.5:1	7100 (1)	NA @ 1 μM	12000 (1)

^a Trifluoroacetate salt. ^b The 2S/2R epimeric ratio was determined by analytical HPLC except where otherwise noted. ^c Abbreviations: thr, human α -thrombin; try, bovine trypsin; NA, not active (less than 10% inhibition at the specified concentration); ND, not determined; SB, slow-binding kinetics. Standard errors are given for *N* experiments (indicated in parentheses). ^d Determined by ¹H NMR by the ratio of the *N*-methyl peak integrals. ^e Slow-binding K_i = 430 ± 110 nM (*N* = 11). ^f IC₅₀ = 630 (*N* = 1). ^g IC₅₀ = 540 ± 50 nM (*N* = 3). ^h Determined by ¹H NMR by the ratio of the α -methine peak integrals.

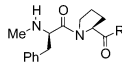
converted to **28** in the usual manner. Ester **28d** was reacted directly with 2-lithiobenzothiazole because the Weinreb amide could not be obtained from the corresponding acid despite our attempts to employ various coupling reagents (BOP, PyBOP, PyBrOP, or BOP-Cl).²⁸

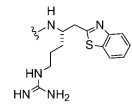
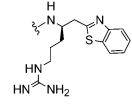
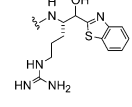
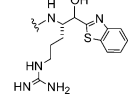
trans-4-Aminomethylcyclohexylglycine derivatives **41** and **42** were prepared by a Strecker reaction (Scheme 4).²⁹ Esterification of acid **41a** followed by Mtr protection of the amino group gave ester **41b**, and reduction of **41b** to the corresponding alcohol followed by oxidation with the Dess–Martin periodinane gave aldehyde **41c**. Reaction of **41c** with sodium cyanide in the presence of ammonium carbonate followed by hydrolysis with 4 M sodium hydroxide provided the desired α -amino acid. This material was protected with a Boc group and coupled to *N*-methoxy-*N*-methylamine to yield Weinreb

amide **41d**, which was converted to a mixture of **41** and **42** via the Weinreb amide route (Scheme 2).

L-Methoxypropylglycine derivative **43** was synthesized via Evans chiral *N*-acyl-2-oxazolidinone chemistry (Scheme 5).³⁰ Alcohol **43a** was oxidized to acid **43b**, which was converted to the oxazolidinone **43c**.³⁰ Lithiation of **43c**, followed by reaction with di-*tert*-butyl azodicarboxylate, provided **43d**, which was hydrolyzed to give hydrazine **43e**. Removal of the Boc groups, reduction of the hydrazine, Boc protection of the amine, and Weinreb amide formation gave **43f**, which was reacted with 2-lithiobenzothiazole. The resulting ketone was reduced to provide alcohol **43g**, which was converted to **43** via the Weinreb amide route (Scheme 2).

2-(4-Aminocyclohexyl)- β -alanines **71** and **72** were prepared by a modified Knoevenagel procedure (Scheme 6).³¹ Knoevenagel condensation of aldehyde **69d** in the

Table 4. Biological Data for Non-Ketone Analogues


compd ^a	R	2 <i>S</i> /2 <i>R</i> ^b	thr <i>K</i> _i , nM ^c	thr IC ₅₀ , nM ^c	try <i>K</i> _i , nM ^c
46		99:1	ND	58000 (1)	ND ^d
47		1:99	ND	63000 (1)	ND ^e
48 ^f		42:1	5300 ± 2500 (6)	48000 (1)	180000 ± 50000 (3)
49 ^f		26:1	1600 ± 200 (3)	17000 (1)	250000 ± 140000 (2)

^a Isolated as a trifluoroacetate salt. ^b Refers to the stereogenic carbon bearing the guanidinopropyl side chain. The 2*S*/2*R* epimeric ratio was determined by analytical HPLC. ^c Abbreviations: thr, human α -thrombin; try, bovine trypsin; ND, not determined. Standard errors are given for *N* experiments, which are indicated in parentheses. ^d IC₅₀ = 32000 nM (*N* = 1). ^e IC₅₀ = 30000 nM (*N* = 1). ^f Enriched in one diastereomer; however, the absolute stereochemistry is unknown.

presence of ammonium acetate provided β -alanine **71a**, which was protected with a Boc group and converted to the Weinreb amide **71b**. Compound **71b** provided **71** and **72** via the Weinreb amide route (Scheme 2).

Epimerization Studies. One can appreciate that the proton on the stereogenic center adjacent to the activated ketone of peptide-based α -ketoheterocycles is somewhat labile such that stereomutation might take place during synthetic processes, biochemical assays, or in vivo experiments. Therefore, it is important to understand the potential for stereomutation, especially under the conditions used for the bioassays. We evaluated the epimerization of thiazole **59** (L-Arg/D-Arg = 98:2), an early lead compound, in the buffers that were used for thrombin (pH 7.40 and 7.85) and trypsin (pH 7.40 and 8.40) inhibition assays (Table 7³²). After 35 min at 37 °C (enzyme assay conditions), some epimerization of the L-arginine to the D-arginine diastereomer was apparent in both buffer systems by analytical HPLC. The L-arginine content of **59**, which was initially 98%, decreased to 92% in the pH 7.85 thrombin buffer and to 93% in the pH 7.4 thrombin buffer, whereas it decreased to 73% in the pH 8.4 trypsin buffer. At pH 7.4, epimerization was slightly faster in the trypsin buffer (87%) than in the thrombin buffer (93%). Similar epimerization results were reported for efegatran (**1b**).^{11b} A solution of **59** in distilled water (pH 6.5) did not epimerize after 3 h at 23 °C but changed to a 73:27 mixture after 16 days. Although **59** epimerized under mildly basic conditions, it is reasonably stable stereochemically under mildly acidic conditions, such as pH 3–4.

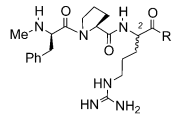
In a separate study, benzothiazole **4** (L-Arg/D-Arg = 98:2) was dissolved in the pH 7.4 thrombin buffer at 37 °C and epimerization was monitored. The L-Arg/D-Arg isomer ratio changed to 70:30 after 0.5 h, 60:40 after 1 h, and 50:50 after 6.5 h. Under these conditions, **59** (L-Arg/D-Arg = 98:2) gave a 70:30 mixture after 0.5 h and a 50:50 mixture after 1 h (and after 6.5 h). Thus, the

L-Arg/D-Arg diastereomer ratio at equilibrium for **4** and **59** is essentially 1:1. On the basis of these epimerization studies, we confidently performed the thrombin and trypsin inhibition assays at pH 7.4 (normal pH of human plasma) within a 30-min time frame.

To approximate in vivo epimerization for the keto-benzothiazoles, we also monitored the rate of equilibration of **3** in rabbit and rat plasma over 120 min at pH 7.4 and 37 °C. In both milieus, a 53:47 mixture of L-Arg/D-Arg epimers, **3:27**, was obtained after 60 min, indicating that **3** would be almost completely epimerized within 1 h under physiological conditions.

Structure–Activity Relationships. A broad range of compounds (**3–77**) was assessed for the inhibition of human α -thrombin and bovine trypsin (Tables 1–6). Compounds **3–77** generally displayed competitive Michaelis–Menten kinetics, although some exhibited slow-binding (i.e., time-dependent) kinetics for thrombin. Hence, the thrombin IC₅₀ values are also given because they are a better comparator for assessing the relative potency of slow-binding inhibitors with Michaelis–Menten inhibitors, since all IC₅₀ values were determined under the same experimental conditions. We included trypsin inhibition as a primary selectivity screen because of trypsin's high structural homology with thrombin. In the X-ray crystal structure of human α -thrombin, 195 out of 259 α -carbons in the B chain occupy topologically equivalent positions relative to bovine trypsin with a root-mean-squared (rms) deviation of 0.82 Å.^{4b} Consequently, good selectivity (i.e., >100-fold) for thrombin over trypsin can be difficult to attain. Trypsin inhibition might present a source of adverse effects following oral administration.^{33,34}

Early in the project, we discovered that the 2-benzothiazole group together with the L-amino acid stereochemistry at P₁, as in **3**, confer excellent thrombin affinity (*K*_i = 0.20 nM) and moderate selectivity over trypsin (16-fold). This finding was investigated further with systematic changes to the P₃, P₂, P₁, and P₁'

Table 5. Biological Data for P₁' Analogues


compd ^a	R	2 <i>S</i> /2 <i>R</i> ^b	thr K _i , nM ^c	thr IC ₅₀ , nM ^c	try K _i , nM ^c
50		5.7:1	85 ± 20 (6)	930 (1)	73 ± 15 (6)
51		99:1	2400 ± 400 (6)	13000 (1)	1300 ± 400 (6)
52		12:1 ^d	200 ± 70 (6)	1,500 (1)	5800 ± 800 (6)
53		7.5:1 ^d	9.6 ± 1 (6)	360 (1)	12 ± 4 (6)
54		4.4:1 ^d	8.1 ± 1.2 (6)	110 (1)	290 ± 40 (6)
55		99:1 ^d	6.2 ± 1.6 (9)	110 (1)	13 ± 7 (7)
56		1.2:1 ^d	15 ± 3 (6)	106 (1)	8.3 ± 0.6 (6)
57		34:1 ^e	2.1 ± 0.5 (8)	19 (1)	1.2 ± 0.4 (4)
58		7.5:1 ^d	9.1 ± 1.0 (3)	112 (1)	6.0 ± 0.7 (3)
59		49:1	4.5 ± 0.2 (3)	120 ± 30 (6)	5.4 ± 2.9 (4)
60		6.7:1 ^d	120 ± 20 (6)	830 (1)	5.0 ± 1.4 (5)
61		10:1 ^e	3.4 ± 1.0 (6)	80 ± 26 (5)	4.4 ± 1.2 (5)
62		9:1 ^e	0.58 ± 0.08 (6)	60 ± 14 (6)	15 ± 3 (9)
63		49:1	0.14 ± 0.01 (6)	5.0 ± 3.0 (2)	2.0 ± 0.5 (5)
64		32:1	0.23 ± 0.03 (5)	3.0 (1)	3.5 ± 1.2 (4)
65		39:1 ^d	0.15 ± 0.05 (5)	7.5 ± 0.5 (2)	1.5 ± 0.3 (3)
66		10:1 ^d	0.37 ± 0.08 (6)	7.0 (1)	5.3 ± 1.6 (3)
67		4:1 ^d	SB ^f	5.0 (1)	0.30 ± 0.10 (4)
68		4.3:1 ^d	1.3 ± 0.1 (3)	38 ± 19 (4)	31 ± 13 (3)
4		8.7:1	2.0 ± 0.9 (9)	45 ± 11 (5)	2.7 ± 1.2 (5)
1b	H	ND	18 ± 4 (12)	85 ± 32 (3)	9.1 ± 3.7 (9)

^a Trifluoroacetate salt. ^b The 2*S*/2*R* epimeric ratio was determined by analytical HPLC, except where otherwise noted. ^c Abbreviations: thr, human α -thrombin; try, bovine trypsin; NA, not active (less than 10% inhibition at the specified concentration); ND, not determined. Standard errors are given for *N* experiments (given in parentheses). ^d Determined by ¹H NMR via integration of the *N*-methyl signals. ^e Determined by ¹H NMR via integration of the α -methine signals. ^f Slow binding $K_i = 0.0070 \pm 0.0022$ nM (2).

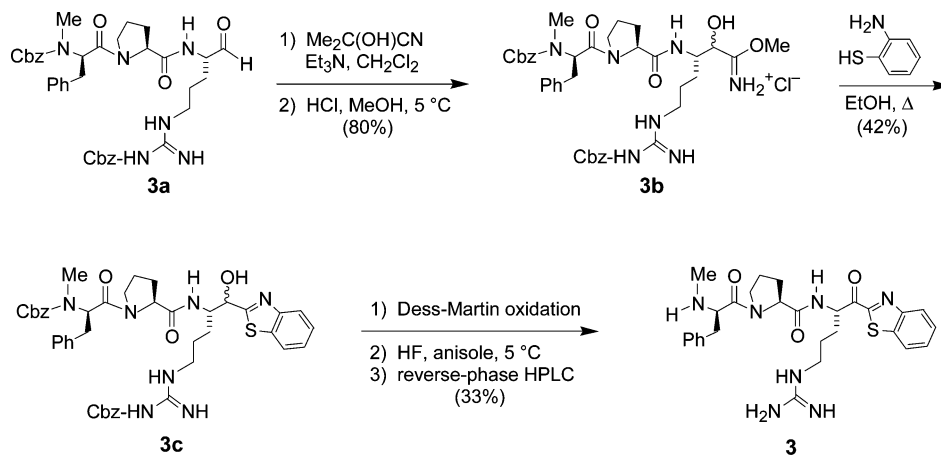
segments of the D-Phe-Pro-Arg-X pharmacophore (Figure 1). Modifications of the P₃ residue were conducted with cognizance of the SAR knowledge base for this

tripeptide motif.^{7a,11} Thus, the D-amino acid stereochemistry and a hydrophobic side chain were generally maintained. The presence of a suitable P₃ residue, such

Table 6. Biological Data for Other Thrombin Recognition Motifs

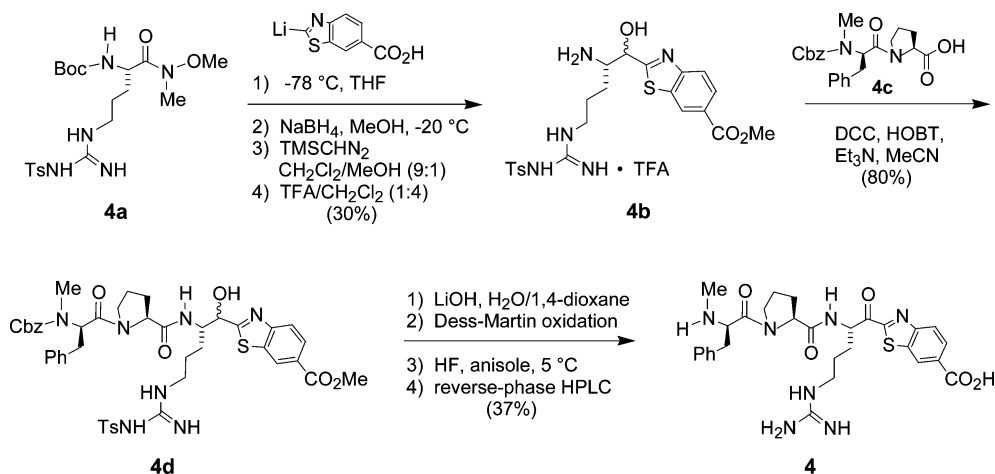
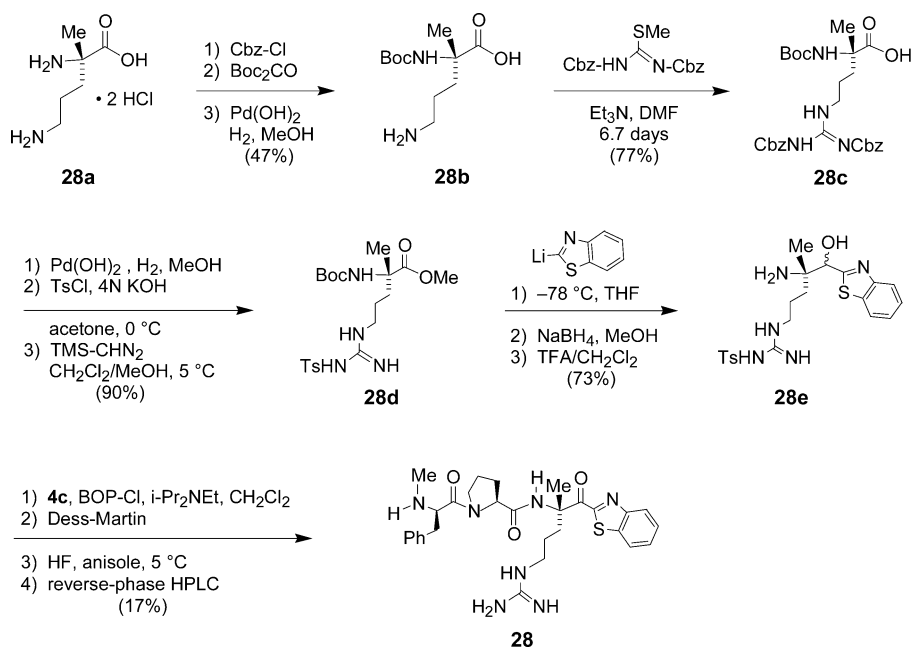
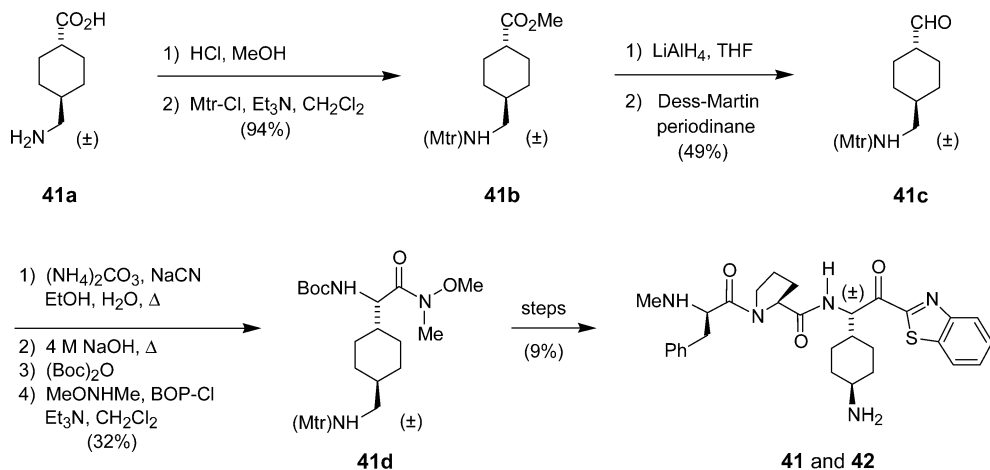
compd ^a	R	2 <i>S</i> /2 <i>R</i> ^b	thr K _i , nM ^c	thr IC ₅₀ , nM ^c	try K _i , nM ^c
69 ^d		1:1	110 ± 30 (9)	1900 ± 1300 (2)	330 ± 70 (6)
70 ^d		1:1	53 ± 3 (6)	460 ± 10 (2)	87 ± 6 (3)
71 ^{d,e}		<i>f</i>	ND	>100000	ND ^g
72 ^{d,e}		<i>f</i>	ND	>100000	ND ^h
73		1.3:1 ⁱ	400 ± 80 (3)	4000 ± 1200 (2)	57 ± 10 (3)
74		1.4:1	16 ± 4 (3)	270 ± 60 (6)	9.4 ± 0.8 (3)
75		13:1	1.4 ± 0.2 (9)	56 ± 22 (4)	16 ± 6 (3)
76		9:1	1.5 ± 0.4 (6)	95 ± 80 (2)	2.7 ± 1.5 (4)
77		99:1	0.78 ± 0.1 (3)	110 ± 30 (6)	2.9 ± 1.1 (2)

^a Trifluoroacetate salt. ^b The 2*S*/2*R* epimeric ratio was determined by analytical HPLC except where otherwise noted. ^c Abbreviations: thr, human α -thrombin; try, bovine trypsin; ND, not determined; SB, slow-binding kinetics. Standard errors are given for *N* experiments (given in parentheses). ^d The relative stereochemistry of the cyclohexyl ring is trans. ^e The absolute stereochemistry of the carbon that bears the cyclohexyl ring is unknown; its configuration is drawn arbitrarily. ^f Compound is essentially a single diastereomer (for **71**, **71/72** = 99:1; for **72**, **71/72** = 1:99). ^g IC₅₀ = 58000 nM (*N* = 1). ^h IC₅₀ = 22000 nM (*N* = 1). ⁱ Determined by ¹H NMR via the ratio of the α -methine peak integrals.

Scheme 1. Imidate Route to **3**

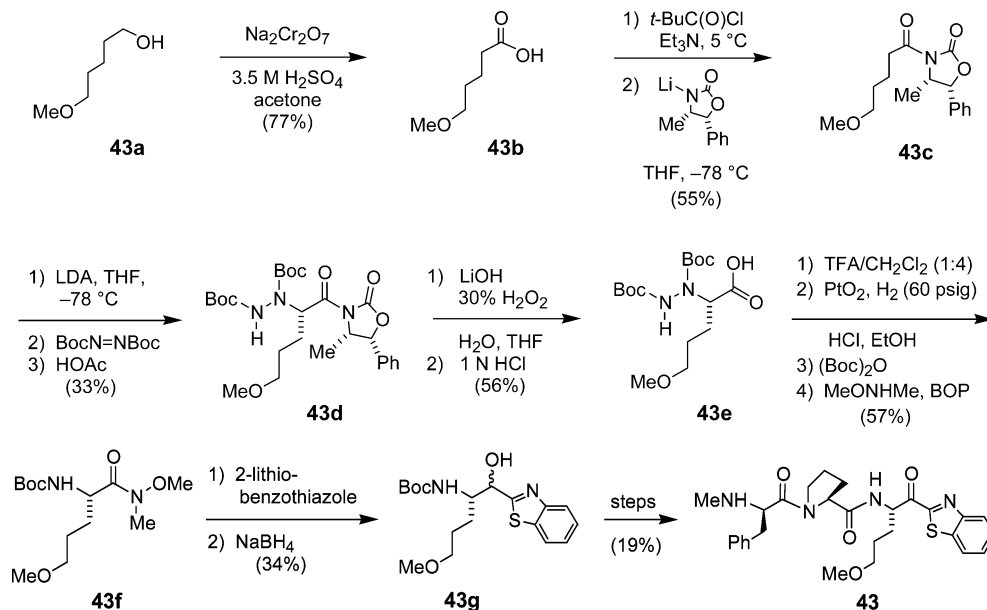
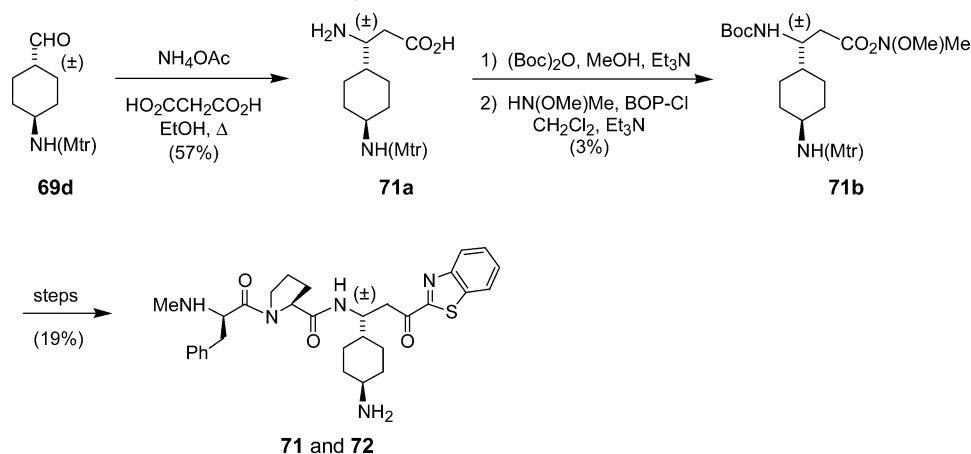
as the D-Phe unit of **3**, is critical for thrombin affinity, as reflected in the lack of potency for **20** (Table 1). Since D-cyclohexylalanine, as in **8**, did not diminish thrombin affinity, the π stacking interaction between a P₃ aryl

group and Trp-215 (Figure 1) can obviously be compensated for by general hydrophobic interactions (i.e., "grease"). This point is also illustrated by results for the D-phenylglycine (**15**) and D-cyclohexylglycine (**16**) ana-

Scheme 2. Weinreb Amide Route to **4****Scheme 3.** Synthesis of L- α -Methylarginine Derivative **28****Scheme 4.** Synthesis of *trans*-4-Aminomethylcyclohexylglycine Derivatives **41** and **42**

logues. Substitution of D-Phe with a 4-fluoro substituent led to a minor improvement in thrombin affinity, whereas perfluorination decreased thrombin affinity (cf. **3** with **6** and **7**). Methyl substitution at the D-Phe stereogenic center was tolerated because there was no

effect on thrombin affinity (cf. **5** with **11**). A basic nitrogen in P₃, which in D-Phe-Pro-Arg thrombin inhibitors is typically hydrogen-bonded to Gly-216 (Figure 1), conferred potent thrombin affinity (cf. **3** with **9** and **10**, as well as **13** with **14** and **19**). Although des-amino

Scheme 5. Synthesis of L-(3-Methoxypropyl)glycine Derivative **43****Scheme 6.** Synthesis of 2-(4-Aminocyclohexyl)- β -alanine Derivatives **71** and **72**

compound **14** is less potent than the corresponding amino derivative **13**, it still had respectable thrombin affinity ($K_i = 1.1$ nM). Alkylation of the N-terminal nitrogen may eliminate slow-binding kinetics, as for **3** or **12** vs **5**. D-Diphenylalanine^{11c} and D-cyclohexylglycine^{11d} derivatives **13** and **16** are particularly noteworthy because they displayed the greatest thrombin affinity of the compounds studied, with thrombin K_i values of 0.000 65 and 0.018 nM, respectively (slow-binding kinetics). Compounds **13** and **16** were also among the most potent inhibitors in terms of thrombin IC_{50} values: 4.5 and 5.3 nM, respectively.

The presence of a suitable P_2 residue, similar to Pro, is important for high thrombin and trypsin affinity, as illustrated by **25** and **26** vs the truncated analogues **21**–**24** (Table 2). Substitution of L-Val for L-Pro led to diminished thrombin affinity and equipotent trypsin activity relative to **3**, whereas substitution with L-homoproline resulted in activity virtually identical to that of **3**. The attached hydrophobic P_3 residue, such as D-Phe, is very important (Table 2). The higher trypsin inhibitory potencies for **22** and **23** relative to **21** may be attributed to reestablishing the hydrogen bond between the Arg $\alpha\text{-NH}$ of the inhibitor and the Ser-214 carbonyl of the β -sheet (Figure 1). Compound **23** is

intriguing as a trypsin inhibitor because of its relatively high affinity ($K_i = 30$ nM) and low molecular weight (387 Da).^{19j,35}

Modifications of the P_1 residue, i.e., the L-Arg moiety of **3**, illustrate the importance of the L-amino acid stereochemistry and the basic functionality for potent thrombin and trypsin activity, especially in the case of transition-state analogues (Table 3). Considering the L-amino acid analogues with reasonable potency, that is, with thrombin inhibition in the nanomolar range, they had significantly higher thrombin and trypsin affinities than did their D-epimer counterparts (cf. **3** with **27**, **32** with **33**, **35** with **36**, and **37** with **38**). Much of the thrombin inhibition attributed to the D-epimers is probably due to the presence of small amounts of the more potent L-epimers. Because of this situation, we methylated the L-arginine stereogenic center to prevent epimerization and provide pure, stable D and L isomers for study. However, this structural change resulted in slow-binding kinetics and a significant decrease in thrombin affinity presumably because of steric factors (cf. **3** with **28**). A similar outcome for α -methyl substitution was reported for the analogous aldehyde series, i.e., D-MePhe-Pro-Arg(α -Me)H.³⁶ N-Methylation of the arginine α -amino group severely affected the thrombin and

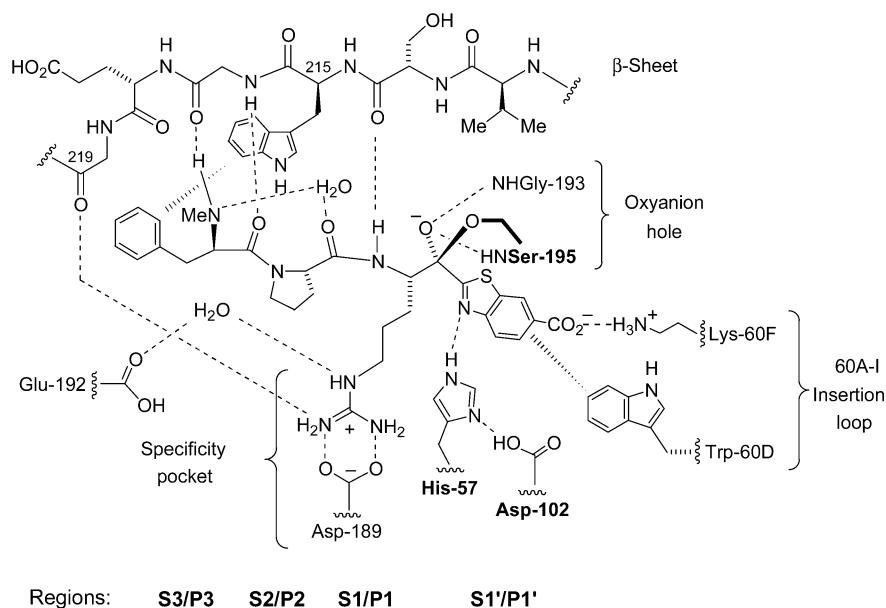


Figure 1. Diagram representing the key interactions between **4** (RWJ-51438) and thrombin.^{15b}

trypsin potency, as would be expected from disruption of a hydrogen bond between the Arg α -NH and the carbonyl group of Ser-216 of the β -sheet (cf. **3** with **29**; Figure 1). Since basic P_1 groups of thrombin inhibitors typically form a strong salt bridge with Asp-189 in the thrombin specificity pocket (Figure 1), it is not surprising that there was a strong correlation between decreasing thrombin affinity and decreasing basicity (cf. **3** with **32**, **37**, and **43–45**). Additionally, extension of the Arg side chain by just one methylene dramatically decreased thrombin affinity (cf. **3** with **30**). The sensitivity of positioning the basic group was also observed in the significantly higher thrombin affinity for 3-amidinophenylalanine **32** relative to 4-amidinophenylalanine **31** and for (*S*)-1-amidinopiperidine derivative **34** relative to its corresponding (*R*)-isomer **35**. Methylation of the amino group of the P_1 Lys side chain caused a dramatic decrease in thrombin and trypsin affinities (cf. **37** with **39**). The *trans*-4-aminomethylcyclohexylglycine derivative **41** displayed weak thrombin affinity ($K_i = 920$ nM) and modest trypsin activity ($K_i = 54$ nM). In the neutral P_1 compounds **43–45**, butyl analogue **44** was essentially devoid of thrombin inhibition, whereas benzyl analogue **45** had very weak thrombin inhibition ($K_i = 7100$ nM). The weak K_i value of 3900 nM for methoxypropylglycine analogue **43** is in stark contrast with the potent K_i of 7 nM reported for a related methoxypropyl derivative in a boronic acid series of thrombin inhibitors.³⁷

Some nonketone analogues, **46–49**, were prepared to ascertain the importance of an activated carbonyl functionality for thrombin inhibition (Table 4). The methylene analogues **46/47** and the alcohol derivatives **48/49** had extremely weak thrombin potency relative to **3**. The somewhat better thrombin affinity of alcohols **48/49** relative to **46/47** might be attributed to the formation of a hydrogen bond with Gly-193 or Ser-195 (Figure 1). The results for non-ketones **46–49** attest to the crucial role of the electrophilic ketone for strong enzyme inhibition, consistent with a transition-state analogue.

Modifications of the activating heterocycle at P_1' , i.e., the benzothiazole moiety of **3**, had a dramatic impact on thrombin affinity (cf. **50–68** and **4**; Table 5). At least two heteroatoms proximal to the carbon bearing the carbonyl group are required for potent activity (cf. **3** with **50** and **51**). Although pyridine derivative **50** contains a π -deficient heterocycle that can activate the adjacent carbonyl, it showed modest potency relative to **3**. Benzothiazole **51** was found to have 12000-fold less thrombin affinity than benzothiazole **3**, indicating the key importance of the heterocyclic nitrogen atom. The significant increase in potency for **3** relative to benzoxazole **55** (30-fold) and *N*-methylbenzimidazoles **53/54** (40/50-fold) may be associated with the relative π electron-withdrawing power of these heterocycles³⁸ and/or a hydrophobic patch for interaction of the sulfur atom on the surface of thrombin (vide infra). Methyl substitution in the imidazole series did not improve thrombin inhibition; however, it did enhance the selectivity for thrombin over trypsin (entries **52–54**). In the thiazole series, substituted thiazoles always exhibited less thrombin inhibition relative to the unsubstituted thiazole (cf. **58–61** with **57**). Moreover, the thiazoles usually exhibited higher affinity for trypsin than for thrombin (entries **57–61**). Benzo-fused thiazoles, oxazoles, and imidazoles consistently had greater thrombin inhibition and more selectivity over trypsin than their non-benzo counterparts. Benzothiazole **3** had 10-fold more thrombin affinity than thiazole **57**, and benzimidazole **54** had 25-fold more thrombin affinity than imidazole **52**. This result may be due to the benzo-fused heterocycles having increased electronic induction, thereby increasing the electrophilicity of the keto group. However, although the thrombin affinity of benzothiazole **3** relative to thiazole **57** increased, the trypsin affinity remained essentially unchanged. We attribute this increase in thrombin affinity and trypsin selectivity to an edge-to-face aromatic-stacking interaction between the benzene ring of the benzoheterocycle and the indole ring of Trp-60D of the thrombin 60A-I insertion loop (Figure 1), which has been observed by X-ray crystallography

(vide infra).¹⁵ Fusion of another phenyl ring to generate a naphthothiazole, as with **62**, did not enhance thrombin affinity relative to **3**. Reduction of the benzothiazole benzene unit caused a 17-fold reduction in thrombin affinity and did not affect trypsin affinity (cf. **3** with **61**), consistent with an aromatic-stacking interaction between the benzoheterocycle and the indole ring of Trp-60D, as saturated hydrophobicity will not effectively replace the planar benzene ring. Substitution at the benzothiazole 6-position with hydroxy, hydroxymethyl, methoxy, and fluoro groups did not significantly affect thrombin affinity (cf. **63–66**). 6-Carboxamido substitution (**67**) led to one of the most potent compounds in terms of thrombin IC₅₀ values, although slow-tight binding kinetics were obtained. Relative to **3**, 6-carbomethoxy (**68**) and 6-carboxy (**4**) substitution caused a 6-fold and 10-fold reduction, respectively, of thrombin affinity in terms of K_i values.

We tested the heterocycle-activated ketone approach with other thrombin recognition motifs (viz. **69**, **70**, **73–77** (Table 6)). Compounds **69** and **70**, ketobenzothiazole analogues of a *N*-methylketoamide inhibitor L-370,518, exhibited only modest thrombin inhibition (K_i values of 110 and 53 nM, respectively) and also lacked selectivity over trypsin, which is in sharp contrast to the results reported for L-370,518 (thrombin K_i = 0.09 nM; trypsin K_i = 5 μ M).³⁹ A molecular modeling study suggested that steric interactions between the 4-aminocyclohexane groups of **69** and **70** and the benzothiazole may be responsible for the modest thrombin potency and that insertion of a methylene spacer between the side chain and the activated carbonyl group would help alleviate the problem. Hence, **71** and **72** were prepared, but they were essentially devoid of thrombin inhibition. Compound **73**, a ketobenzothiazole analogue of a selective boroarginine derivative,⁴⁰ had only weak thrombin inhibition and no selectivity over trypsin. More encouraging results were obtained with **74–77**, which had thrombin K_i values in the range 1.4–16 nM. Compounds **74–76** are analogues of orally bioavailable arginals,⁴¹ and **77** is an analogue of an orally bioavailable, selective agmatine⁴² derivative. Of these ketobenzothiazoles, only **75** exhibited selectivity over trypsin, albeit by just a factor of 11.

The in vitro antithrombotic activity of selected compounds from **3–68** was assessed by the inhibition of gel-filtered platelet (GFP) aggregation induced by α -thrombin (Table 8). GFP preparations allow the determination of antiplatelet activity in the absence of plasma coagulation factors and fibrinogen. The most potent compound from this group was L-homoproline derivative **26**, with an aggregation IC₅₀ value of 10 nM (thrombin K_i = 0.34 nM). In comparison, reference thrombin inhibitor efgatran (**1b**) had an IC₅₀ value of 83 nM. Compounds with the P₃ substituent modified to D-cyclohexylalanine **12**, D-phenylglycine **15**, D-cyclohexylglycine **16**, and L-aspartate **75** also displayed potent activity, with GFP aggregation IC₅₀ values of less than 20 nM. Higher thrombin affinity did not necessarily translate into more potent inhibition of aggregation (cf. **3** with **75** and **77**). Lead compounds **3**, **4**, and **68** inhibited GFP aggregation with relatively potent IC₅₀ values of 32, 41, and 39 nM, respectively.

Table 8. Gel-Filtered Platelet Aggregation and Blood Pressure Effect in Guinea Pigs^a

cmpd	thr K _i , nM ^b	GFP aggr IC ₅₀ , nM ^c	Δ BP% @ dose, mg/kg ^d
1b	18 \pm 4 (12)	83 \pm 28 (9)	–21 @ 10
3	0.18 \pm 0.02 (18)	32 \pm 6 (10)	–85 @ 3
4	2.0 \pm 0.9 (6)	41 \pm 19 (4)	–32 @ 10
8	0.18 \pm 0.03 (4)	28 \pm 1 (2)	–49 @ 3
10	24 \pm 4 (3)	46 \pm 9 (3)	–36 @ 10
12	0.36 \pm 0.09 (4)	16 \pm 4 (4)	–47 @ 10
13	SB	43 \pm 14 (3)	–54 @ 3
14	3.1 \pm 0.6 (6)	29 \pm 9 (4)	–25 @ 3
15	0.46 \pm 0.05 (6)	17 \pm 6 (3)	–63 @ 3
16	ND	17 \pm 3 (2)	–21 @ 3
19	3.1 \pm 1.2 (3)	ND	–70 @ 10
25	21 \pm 7 (6)	180 \pm 18 (2)	–47 @ 3
26	0.34 \pm 0.05 (6)	10 \pm 1 (2)	–45 \pm 15 @ 3 (2)
37	38 \pm 5 (3)	ND	–45 @ 3
38	210 \pm 10 (3)	ND	–41 @ 3
39	3700 \pm 600 (3)	5200 \pm 1800 (2)	–16 @ 1
52	200 \pm 70 (6)	230 \pm 40 (3)	–68 \pm 4 @ 10 (2)
54	8.1 \pm 1.2 (6)	59 \pm 16 (2)	–30 @ 3
61	3.4 \pm 1.0 (6)	22 \pm 5 (5)	–70 @ 10
62	0.58 \pm 0.08 (6)	ND	–51 @ 10
63	0.14 \pm 0.01 (6)	ND	–44 @ 3
64	0.23 \pm 0.03 (5)	ND	–34 @ 3
65	0.15 \pm 0.05 (5)	ND	ND
68	1.3 \pm 0.1 (3)	39 \pm 13 (7)	–16 @ 10
69	110 \pm 30 (9)	76 \pm 22 (4)	–25 @ 3
70	53 \pm 3 (6)	120 \pm 28 (4)	ND
74	16 \pm 4 (3)	47 \pm 14 (3)	–39 @ 10
75	1.4 \pm 0.2 (9)	16 \pm 2 (2)	ND
76	1.5 \pm 0.4 (6)	37 \pm 17 (2)	–64 @ 10
77	10 \pm 2 (6)	34 \pm 13 (3)	–30 @ 20

^a Abbreviations: ND, not determined; SB, slow-binding kinetics; thr, human α -thrombin; GFP aggr, gel-filtered platelet aggregation; BP, blood pressure. The number of experiments (*N*) is in parentheses. ^b K_i values (mean \pm standard error) for thrombin inhibition. ^c IC₅₀ values (mean \pm standard error) for inhibition of human platelet aggregation. ^d Percent change in blood pressure in guinea pigs at the given dose (iv).

Our intent was to assess selected compounds in vivo for their anticoagulant/antithrombotic activity. As a prelude, we examined the general cardiovascular effects of certain lead compounds on intravenous (iv) administration to anesthetized guinea pigs.⁴³ Unfortunately, **3** and some of its analogues elicited pronounced hypotension and electrocardiogram (ECG) effects (Table 8).^{43b} Hypotensive side effects have been reported in other series of thrombin inhibitors,^{40,44} and **1b** (efegatran) in our hands caused hypotension at a 10-fold higher dose than the dose of **3** (30 vs 3 mg/kg). Thus, we tested representative analogues of **3** for their hypotensive effects. The P₁ Arg side chain was not the primary cause of hypotension because the corresponding Lys and 4-aminocyclohexylglycine analogues, **37** and **69**, also caused a drop in blood pressure of 45% and 25% at 3 mg/kg, respectively. Many modifications, at the P₃ (**8**, **12–16**, and **19**), P₂ (**25**, **26**), and P₁' (**52**, **54**, **61–65**, **68**) positions, caused a substantial decrease in blood pressure. Hypotension was also induced by thrombin recognition motifs other than D-Phe-Pro, such as in **74–77**. Fortunately, carboxylic acid and carboxylic ester analogues **4** and **68** (methyl ester of **4**) displayed significantly diminished hypotension and ECG effects relative to **3**, allowing for their use in subsequent in vivo studies (vide infra).⁴⁵

Several agents and pathways were evaluated as possible causes of the hypotension and ECG effects of **3** and its analogues, including nitric oxide, bioactive amines, cholinergic activation, and activation of the complement cascade. We especially suspected the comple-

Table 9. Inhibition of Thrombin Relative to Other Serine Proteases

cmpd	thr K_i , nM ^a	selectivity ratio (K_i other/ K_i thr) ^b						
		trypsin	fXa	plasmin	prot Ca	SK	tPA	uPA
4	2.0 ± 0.9 (9)	1.4	600	390	2400	210	21	8500
68	1.3 ± 0.1 (3)	24	380	110	1800	760	45	1800
3	0.2 ± 0.02 (30)	16	2400	12000	19000	6300	330	23000
1b (efegatran)	18 ± 4 (12)	0.5	5300	28	72	72	78	130
argatroban	9.9 ± 0.7 (7)	470	47000	39000	54000	>10 ⁵	37000	10 ⁶

^a K_i values (mean ± standard error) for thrombin inhibition; the number of experiments (N) is in parentheses. ^b Selectivity is defined as the ratio of the K_i value of the serine protease over the K_i value for thrombin. For the original K_i data, see Supporting Information. Abbreviations: thr, thrombin; fXa, activated factor X; tPA, two-chain tissue-type plasminogen activator; prot Ca, activated protein C; SK = streptokinase; uPA, two-chain urokinase-type plasminogen activator.

Table 10. In Vivo Efficacy in Dogs and Rabbits and Effect on Blood Pressure in Guinea Pigs

cmpd	GP hypotension ^a		dog A-V shunt ^b			rabbit DVT ^{b,c}		
	N	ED ₋₂₅ (mg/kg)	N	ED ₅₀ (mg/kg)	safety ratio ^d (ED ₋₂₅ :ED ₅₀)	N	ED ₅₀ (mg/kg, iv)	safety ratio ^d (ED ₋₂₅ :ED ₅₀)
3	5	0.9 ± 0.5	3	0.46 ± 0.10	2	3	0.25 ± 0.03	4
4	4	13.0 ± 6.8	3	0.14 ± 0.07	93	3	0.43 ± 0.14	30
68	2	13.4 ± 2.1	3	0.47 ± 0.05	29	3	0.35 ± 0.12	38
1b	5	28.6 ± 1.6	3	0.66 ± 0.16	43	3	0.21 ± 0.19	136

^a Hypotensive response in anesthetized guinea pigs (GP). ED₋₂₅ is the dose (iv) for eliciting a 25% decrease in blood pressure ($N = 3$). ^b Dog arteriovenous shunt model. ED₅₀ is the dose (iv) that reduces thrombus weight accumulation on a silk fiber by 50%. ^c Rabbit deep vein thrombosis model. ED₅₀ is the dose (iv) that elicits a 50% reduction of thrombus formation ($N = 3$). ^d Cardiovascular safety estimation, which is based on a comparison of the hypotensive response in anesthetized guinea pigs to the anticoagulant/antithrombotic response in dogs or rabbits.

ment cascade because it was implicated as the source of hypotension associated with DuP-714, a D-Phe-Pro-based boroarginine thrombin inhibitor that turned out to inhibit complement factor I, as well.⁴⁰ Ultimately, none of these mechanisms proved to be responsible, and the cause of the cardiovascular side effects remains unknown. For each possibility, a specific inhibitor or receptor antagonist was given prior to intravenous administration of **3** and blood pressure was monitored. Nitric oxide was ruled out because L-NAME,⁴⁶ an inhibitor of nitric oxide synthesis, did not prevent the hypotension. H1 and H2 histamine receptors were ruled out because suitable antagonists did not prevent hypotension.⁴⁷ Blockade of cholinergic activation with atropine did not prevent hypotension.⁴⁸ Inhibition of complement with tranexamic acid⁴⁹ and depletion of the factors in the complement cascade with cobra venom factor⁵⁰ did not prevent hypotension. In addition, acute, homologous desensitization did not occur.

Assessment of Advanced Leads. We evaluated **3**, **4**, and **68**, as well as the reference standards efegatran (**1b**) and argatroban, for selectivity vs seven important enzymes: trypsin, factor Xa, plasmin, activated protein C, streptokinase, tissue-type plasminogen activator (tPA), and urokinase-type plasminogen activator (uPA) (Table 9). Although **3**, **4**, and **68** are not as selective as argatroban,^{45b} they still show some worthwhile selectivity. Argatroban has a selectivity ratio of 470-fold in favor of thrombin vs trypsin inhibition, whereas **3**, **4**, and **68** have modest selectivities at best: 16-, 1.4-, and 24-fold, respectively. Generally speaking, poor selectivity for thrombin over trypsin has been observed for inhibitors with a D-Phe-Pro-Arg motif. Nevertheless, the selectivity for **3**, **4**, and **68** is better than that for efegatran (try/thr = 0.5).^{11a}

The in vivo anticoagulant/antithrombotic activity of **3**, **4**, and **68** was assessed in two different animal models of thrombosis (iv administration): the canine arteriovenous (AV) shunt model and the rabbit deep vein thrombosis model (Table 10).¹⁶ Blood clots (thrombi)

generated in the canine model contain both platelets and fibrin, whereas the thrombi generated in the rabbit model are mainly comprised of fibrin. In the canine arteriovenous shunt model (Figure 2), **4** was significantly more potent than the other compounds, with an ED₅₀ value of 0.14 mg/kg (dose needed to elicit a 50% inhibition of thrombus formation). Compounds **3**, **68**, and efegatran (**1b**) had ED₅₀ values of 0.46, 0.47, and 0.66 mg/kg, respectively. In addition, **3**, **68**, and efegatran at a 1 mg/kg dose, as well as **4** at a 0.3-mg/kg dose, had no effect on platelet counts, blood pressure, or heart rate. In the rabbit deep vein thrombosis model (Figure 3), **3**, **4**, **68**, and efegatran had ED₅₀ values of 0.29, 0.30, 0.41, and 0.13 mg/kg, respectively.

We needed to estimate the cardiovascular side effect liability of the lead compounds relative to their anti-thrombotic efficacy. By way of a working therapeutic index, we calculated a ratio that compares the ED₅₀ values of **3**, **4**, **68**, and efegatran in each efficacy model to the guinea pig hypotensive ED₋₂₅ values, which reflect the dose needed to elicit a 25% reduction in blood pressure (Table 10). The resulting "safety ratios" allowed the lead compounds to be ranked. The safety ratios using the dog AV shunt model for **4** and **68** were 93 and 29, respectively, which is a meaningful improvement over **3** (safety ratio = 3). These ratios compare favorably with that for efegatran (safety ratio = 43). Similarly, safety ratios using the rabbit model for **4** and **68** were 30 and 38, whereas **3** had a safety ratio of only 4. Consequently, benzothiazole-6-carboxylic acid **4** was deemed to have a favorable safety ratio, or therapeutic index.

Blood samples taken after an iv dose of 1 mg/kg of **4** in anesthetized rats were used to determine percent plasma thrombin inhibition and to extrapolate drug concentration (μ M). Compound **4** was found to have an iv plasma $t_{1/2}$ of 25 ± 7 min. Conscious rats were dosed with 10 mg/kg of **4** by gavage, and an oral $t_{1/2}$ of 60 ± 16 min and oral bioavailability of only 3 ± 1% were determined. As a consequence of the poor oral bioavail-

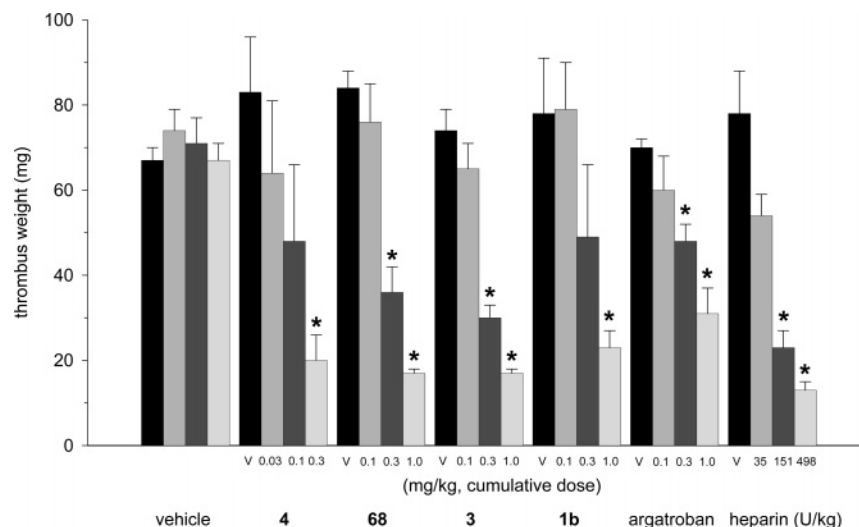


Figure 2. Effects of **4**, **68**, **3**, efegatran (**1b**), argatroban, and heparin on thrombus weight in the canine arteriovenous shunt model. Values are mean (\pm standard error) thrombus weight for $N \geq 3$ for each group. The thrombus weight was determined following 15 min of exposure to shunt flow at each dose. Doses were administered as a bolus plus infusion over the 20 min shunt flow period. The asterisk (*) indicates $p < 0.05$; i.e., the value is significantly different from the control thrombus weight.

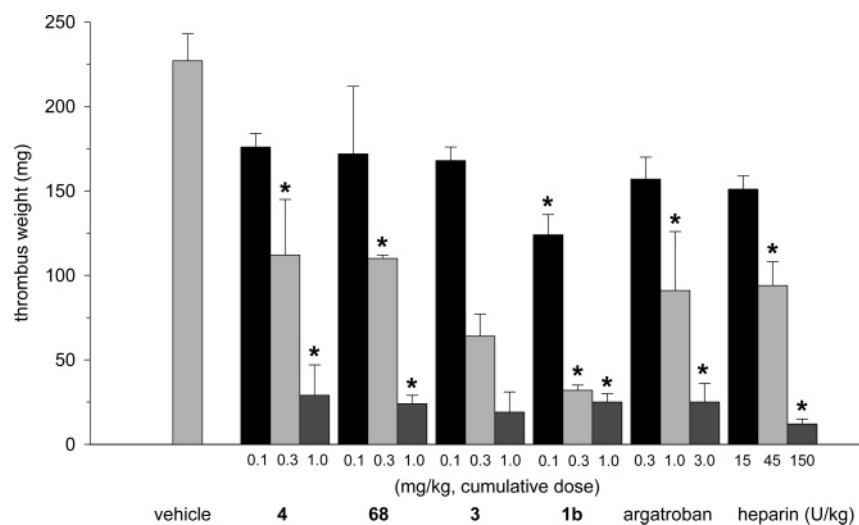


Figure 3. Effects of **4**, **68**, **3**, efegatran (**1b**), argatroban, and heparin on thrombus weight in the rabbit deep vein thrombosis model. Vehicle and each dose of compound were tested in separate groups of animals. Values are mean (\pm standard error) of percent inhibition of thrombus weight. The asterisk (*) indicates $p < 0.05$; i.e., the value is significantly different from the control thrombus weight. The number of experiments (N) was 11 for the vehicle and as follows for the test compounds: **4**, $N = 1$ for 0.1 mg/kg, $N = 3$ for 0.3 and 1 mg/kg; **68**, $N = 3$ for 0.1, 0.3, and 1.0 mg/kg; **3**, $N = 7$ for vehicle, $N = 3$ for 0.1, 0.3, and 1 mg/kg; **1b**, $N = 3$ for 0.1, 0.3, and 1 mg/kg; argatroban, $N = 3$ for 0.3, 1, and 3 mg/kg; heparin, $N = 4$ for 10, 30, and 100 U/kg bolus + 50% dose/20-min infusion (iv).

ability of **4**, there was a lack of interest in moving the compound forward into preclinical development. In this regard, it is interesting to note that a closely related α -ketothiazole thrombin inhibitor exhibited reasonably good oral bioavailability in rats ($F = 23\%$).¹⁸¹

X-ray Crystallography and Molecular Modeling.

We have reported on the X-ray crystal structures of the ternary complexes of **3**^{15a} and **4**^{15b} with thrombin–hirugen (Figure 4).⁵¹ Compounds **3** and **4** are structurally analogous to PPACK (D-Phe-Pro-Arg-CH₂Cl), but they have a methyl group on the N-terminus and a 2-benzothiazole instead of a chloromethyl group. The overall interactions for the D-Phe-Pro-Arg segments in the complexes of **3** and **4** are similar to those observed in PPACK–thrombin (Figure 1).⁴ Both inhibitors form a hemiketal adduct between the Ser-195 hydroxyl and the arginine carbonyl, and the tripeptide motif (P₃–P₂–

P₁) has the standard interactions previously observed in thrombin–inhibitor complexes of this type. However, the benzothiazole binds in an interesting manner at the S₁' subsite, which is mainly defined by His-57, Tyr-60A, Trp-60D, and Lys-60F. The S₁' subsite of thrombin, dominated by Lys-60F,⁵² can accommodate smaller side chains as observed from the P₁' residues of several natural substrates.⁵³ These residues include Gly and Thr and, in some cases, apolar residues, such as Val of fibrinogen A, Leu-13 of protein C, and Ile-153 and Ile-37 of factor VII and factor XI, respectively.^{53d,e} The steric interactions between substrates with Lys-60F in the S₁' subsite create a preference for small P₁' residues.^{4,53} The benzothiazole rings of **3** and **4** hydrogen-bond within the S₁' subsite via their nitrogen atoms to His-57 and stack in a face-to-edge manner with the indole ring of Trp-60D (Figure 1). Consequently, the amino group of Lys-

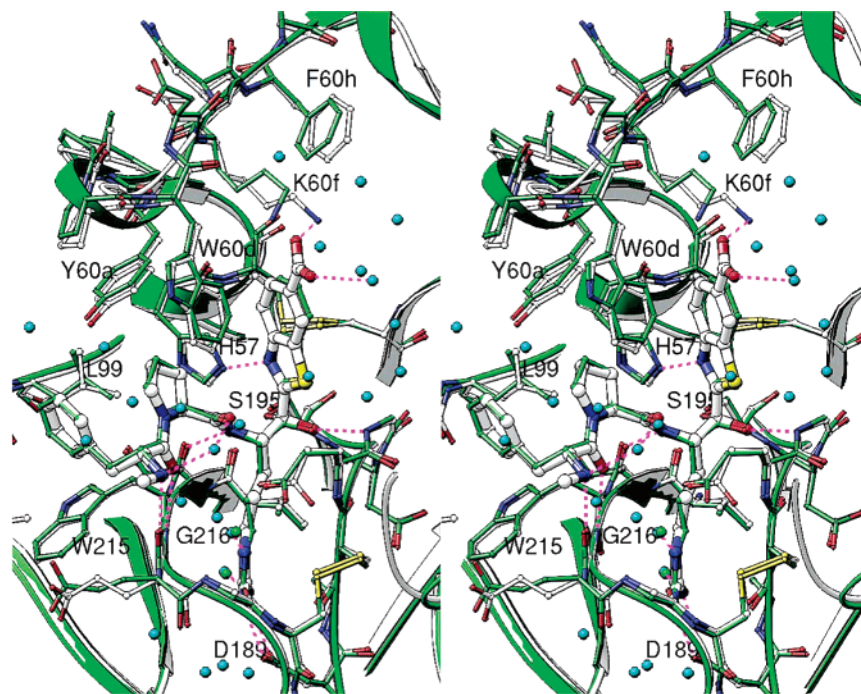


Figure 4. Stereoview of the **4**-thrombin complex (white) overlapped with **3**-thrombin complex (green). Hydrogens were omitted for clarity. Steric interactions with the carboxylic acid moiety of **4** perturb the 60A-I insertion loop relative to **3**-thrombin.

60F in both structures does not form a hydrogen bond with the carbonyl oxygen of His-57. Usually, this hydrogen bond is formed when the S_1' subsite is either unoccupied or occupied by a small residue such as Gly.⁴ Remarkably, **3** is a very potent thrombin inhibitor even though the benzothiazole ring displaces the side chain of Lys-60F from its normal, extended position such that the aminobutyl group is folded into a U-shaped gauche conformation (rmsd of side chain is 1.6 Å). In contrast, the carboxylic acid substituent on the benzothiazole ring of **4** forms a salt bridge with the NZ atom of Lys-60F, thereby drawing it out into an extended anti conformation. It also hydrogen-bonds with a water molecule and forms a salt bridge with the NZ atoms of the symmetry-related residues Lys-236 and Lys-240. Steric interactions with the carboxylic acid moiety of **4** perturb the 60A-I insertion loop relative to **3**-thrombin (Figure 4). Whereas the nonbonded distance between the benzothiazole and the Trp-60D of **4**-thrombin is shorter, leading to stronger van der Waals interactions, the remaining residues are more distant. Apparently, the advantage in binding energy that would be conferred by the salt bridge between Lys-60F NZ and the carboxylic acid of **4** is more than offset by perturbations in the enzyme from steric interactions such that the binding affinity of **4** ($K_i = 2$ nM) is reduced 10-fold relative to that of **3** ($K_i = 0.2$ nM).

The SAR data for **3**-**77**, along with the X-ray crystallographic evidence with **3** and **4**, suggest that the improved affinity and selectivity relative to aldehyde **1b** (efegatran) may be primarily due to two factors: (1) the relative π -electron-withdrawing power of the benzothiazole group and (2) the edge-to-face aromatic-stacking interaction between the benzothiazole phenyl group of **3** and the indole ring of Trp-60D. However, we sought to determine if there might be some additional factors that could contribute to the increased affinity/selectivity of **3** relative to aldehyde **1b** (efegatran).

Hence, we employed computer modeling to compare the potential interactions between **3** and the active sites of thrombin and trypsin with the aid of Goodford's GRID program.⁵⁴ A three-dimensional grid of points (0.5 Å cubes) was generated that encompassed the entire active-site region of both enzymes. Probes possessing the characteristics of various atom types (e.g., hydrophobic, polar, H-bonding, etc.) were placed at each grid point, and the interaction energies with thrombin and trypsin were calculated. These energy fields were then contoured and compared to locate energetically favorable regions or "hot spots" that would favor a particular atom type of an inhibitor in thrombin over trypsin. The hydrophobic aromatic CH probe contoured at -2 kcal proved to be particularly revealing (Figure 5). In thrombin (panel A), the energy contour passes directly through the thiazole ring of **3** and almost completely envelops the sulfur atom, whereas in trypsin (panel B) the thiazole ring and its sulfur atom are left completely exposed, which is energetically less favorable. In contrast, a similar energy difference between these hydrophobic energy contours is not possible for aldehyde **1b** (efegatran). This viewpoint is supported by observations that **3** has better affinity and selectivity than benzoxazole **55** and benzimidazole **53**, and by the increased affinity and selectivity of *N*-methylbenzimidazole **54** relative to benzimidazole **53** (Table 5). Although the increased affinity and selectivity of **3** may be mostly due to the aromatic-stacking interaction with Trp-60D of the thrombin 60A-I insertion loop, it may also be partly due to a hydrophobic interaction between the thiazole ring of **3** and a hydrophobic patch on the surface of thrombin. This binding mechanism for peptidyl α -ketoheterocycle inhibitors and human thrombin differs somewhat from the binding mechanisms reported for human neutrophil elastase¹⁷ and human mast cell tryptase.^{19j} In the case of neutrophil elastase, a determining factor for high affinity appears to be hydrogen

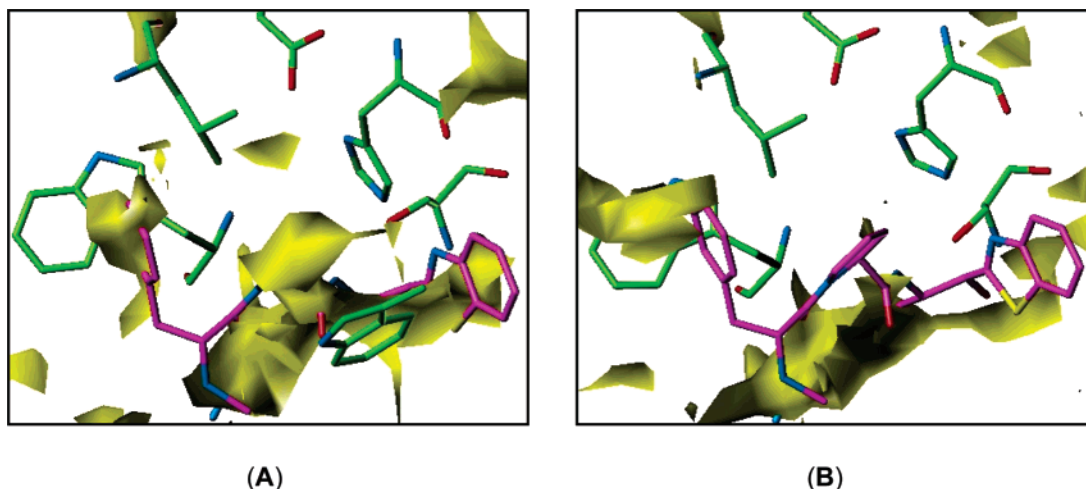


Figure 5. GRID contours for aromatic CH probe (-2 kcal) of **3** bound to thrombin (A) and trypsin (B). In thrombin (A), the energy contour passes directly through the thiazole ring of **3** and almost completely envelops the sulfur atom, whereas in trypsin (B) the thiazole ring and its sulfur atom are left completely exposed, which is energetically less favorable.

bonding between the sp^2 -hybridized nitrogen of the heterocycle and the $N\epsilon$ of His-57.¹⁷ In the case of trypsin, a determining factor for high affinity appears to be the electrophilicity of the heterocycle-activated ketone and/or a hydrophobic interaction with the Cys-42/Cys-58 disulfide bond.^{19j}

Conclusion

We have applied structure-based drug design to the discovery of reversible active-site-directed thrombin inhibitors. Our efforts led to a series of potent α -keto-heterocycle inhibitors primarily based on the D-Phe-Pro-Arg motif (**3–45**, **50–72**). Thrombin inhibition K_i values as potent as 0.000 65 nM (**13**) were obtained, and several compounds had subnanomolar affinities. We extended the α -keto-heterocycle approach to other thrombin recognition motifs (**73–77**) to obtain thrombin K_i values in the range 0.7–400 nM. Compound **3** and several of its analogues caused hypotension and ECG effects in guinea pigs, which were significantly diminished by introducing a carboxylic acid (**4** and **12**) or a carboxylic ester (**68**) onto the benzothiazole.⁵⁵ Benzothiazolecarboxylic acid **4** was efficacious in two animal models of thrombosis, and its therapeutic index compared favorably with that of efegatran (**1b**). However, since **4** has a low oral bioavailability in rats ($F = 3\%$), its clinical use would be limited to parenteral administration. The crystallographic structure of a complex between **4** and thrombin reveals novel interactions in the S_1' region, where the carboxylic acid moiety appended to the benzothiazole forms a salt bridge with the side chain of Lys-60F. Surprisingly, formation of the salt bridge did not result in enhanced thrombin affinity, presumably because of perturbation of the enzyme to accommodate the carboxylic acid group. The SAR data for **3–77**, along with the X-ray crystallographic evidence for **3** and **4**, suggest that their improved affinity/selectivity relative to aldehyde congener **1b** may be primarily due to two factors: (1) the relative π -electron-withdrawing power of the benzothiazole group and (2) the edge-to-face aromatic stacking interaction between the benzothiazole benzene ring of **3** and the indole of Trp-60D. In addition, computational analysis with the GRID program suggests that the improved affinity/

selectivity for **3** may be due to interactions of the benzothiazole sulfur atom with a hydrophobic patch on the surface of thrombin. This binding mechanism for **3** and thrombin differs somewhat from those for peptide α -ketoheterocycles and human neutrophil elastase¹⁷ or human mast cell tryptase.^{19j}

Experimental Section³²

General Information and Procedures. Commercially available reagents were used without purification unless specifically necessary. All reactions were conducted under argon or nitrogen in rigorously dried solvents with magnetic stirring at room temperature unless noted otherwise. All glassware used in the lithiation experiments was flame-dried while assembled with an argon purge, and all butyllithium reagents were assayed immediately before use by titration with 1-pyreneacetic acid.⁵⁶ A pH meter was used to monitor pH adjustments. Multiple extractions are designated within parentheses; for example "(3 \times)" indicates three extractions. Solutions and residues were never heated above 40 °C while concentrating in vacuo. Normal-phase preparative chromatography was performed on an Isco Combiflash Separation System Sg 100c equipped with a Biotage FLASH Si 40M silica gel cartridge (KP-Sil silica, 32–63 μ m, 60 Å; 4 cm \times 15 cm), eluting at 35 mL/min with detection at 254 nm. Reverse-phase preparative chromatography was performed on a Waters Delta-Prep 3000 HPLC equipped with three PrepPak reverse-phase cartridges connected in series (Bondapak C-18; 40 mm \times 300 mm; 15–20 μ m, 125 Å), eluting at 40 mL/min with detection at 220 nm unless noted otherwise; gradient elutions were generally conducted over a 60-min period. Reverse-phase chromatography fractions were lyophilized on a FTS Systems Flexi-Dry MP lyophilizer. Melting points were determined on a Thomas-Hoover apparatus calibrated with a set of melting point standards. Optical rotations were measured on a Perkin-Elmer 241 polarimeter at the sodium D line ($\lambda = 589$ nm) in MeOH (c 1.00) unless noted otherwise. Infrared spectra were recorded on a Nicolet SX-60 spectrometer in KBr pellets with a resolution of 4 cm^{-1} . 1H NMR spectra were acquired at 300.14 MHz on a Bruker Avance-300 spectrometer in CD_3OD unless indicated otherwise, using Me_4Si as an internal standard. NMR abbreviations used were the following: s, singlet; d, doublet; dd, doublet of doublets; t, triplet; m, multiplet; br, broad; ov, overlapping. ^{13}C NMR spectra were acquired at 125.76 MHz at 40 °C on a Bruker Avance-500 spectrometer. HPLC analysis was performed on a Hewlett-Packard series 1100 HPLC instrument, eluting with a gradient of water/MeCN/TFA (from 10:90:0.2 to 90:10:0.2) over 4 min with a flow rate of 0.75 mL/min on a Kromasil C18 column (50 mm \times 2.0

mm; 3.5 μm particle size) or on a Supelcosil ABZ+Plus column (50 mm \times 2.1 mm; 3.0 μm particle size) at 32 °C. Signals were recorded simultaneously at 220, 254, and 305 nm with a diode array detector; purity is reported for the 220 nm signal. Electrospray (ES) mass spectra were obtained on a Micromass Platform LC single quadrupole mass spectrometer in the positive mode. Accurate mass determination (HRMS) was performed on an Autospec E high-resolution magnetic sector mass spectrometer tuned to a resolution of 6 K. The ions were produced in a fast atom bombardment (FAB) source at an accelerating voltage of 8 kV. Linear voltage scans were collected to include the sample ion and two poly(ethylene glycol) ions, which were used as internal reference standards. Elemental analysis and Karl Fischer water (KF) analysis were obtained from Robertson Microlit Laboratories, Inc., Madison, NJ. Abbreviations used were the following: Boc = *tert*-butoxycarbonyl; BOP-Cl = bis(2-oxo-3-oxazolidinyl)phosphonic chloride; BOP reagent = benzotriazol-1-yloxytris(dimethylamino)phosphonium hexafluorophosphate; Cbz = benzyloxycarbonyl; DBU = 1,8-diazabicyclo[5.4.0]undec-7-ene; DCC = dicyclohexylcarbodiimide; DIBAL = diisobutylaluminum hydride; DMAP = 4-(dimethylamino)pyridine; DMF = *N,N*-dimethylformamide; DMSO = dimethyl sulfoxide; EtOAc = ethyl acetate; Fmoc = 9-fluorenylmethylcarbonyl; HOAc = glacial acetic acid; HOBT = 1-hydroxybenzotriazole hydrate; Mtr = 4-methoxy-2,3,6-trimethylbenzenesulfonyl; PyBrOP = bromotris(pyrrolidino)phosphonium hexafluorophosphate; TFA = trifluoroacetic acid; THF = tetrahydrofuran.

(1S)- and (1R)-N-Methyl-D-phenylalanyl-N-[4-[(aminoiminomethyl)amino]-1-(2-benzothiazolylcarbonyl)butyl]-L-prolinamide (3 and 27). Imidate Route Starting with a Tripeptidyl Aldehyde (Scheme 1). A mixture of tripeptide aldehyde **3a**^{1a} (9.92 g, 14.5 mmol), CH_2Cl_2 (48 mL), acetone cyanohydrin (4.0 mL, 43.4 mmol), and triethylamine (1.2 mL, 8.7 mmol) was stirred for 3 h. An additional portion of acetone cyanohydrin (1.3 mL, 14.2 mmol) was added followed by another hour of stirring. The mixture was concentrated in vacuo and partitioned between water (125 mL) and EtOAc (125 mL). The resulting organic layer was washed with water (2 \times) and brine, dried (Na_2SO_4), and concentrated in vacuo. The residue was triturated with hexane (3 \times) and the resulting solid was dried in vacuo to give the crude cyanohydrin intermediate (9.73 g, 94%) as an off-white foam.

Gaseous HCl (51 g) was bubbled into a solution of the cyanohydrin (9.3 g, 13.1 mmol) and anhydrous MeOH (200 mL) at -50 to -70 °C under an atmosphere of argon over 1.5 h. The reaction mixture was placed in a refrigerator at 0 °C for 2 days, transferred to a separatory funnel under argon, and added dropwise at 0–6 °C to a stirred mixture of water (700 mL), EtOAc (250 mL), and NaHCO_3 (159 g, 1.4 mol). The pH of the quenching solution was not allowed to go below pH 6.8. Additional portions of water and NaHCO_3 were added (as dictated by the measured pH) until the reaction mixture was neutralized. The resulting mixture was filtered through a filter agent, and the filtrate was extracted with EtOAc (3 \times). The combined organic layers were washed with brine, dried (Na_2SO_4), and concentrated in vacuo to give the imidate **3b** (7.51 g, 74%) as an off-white foam.

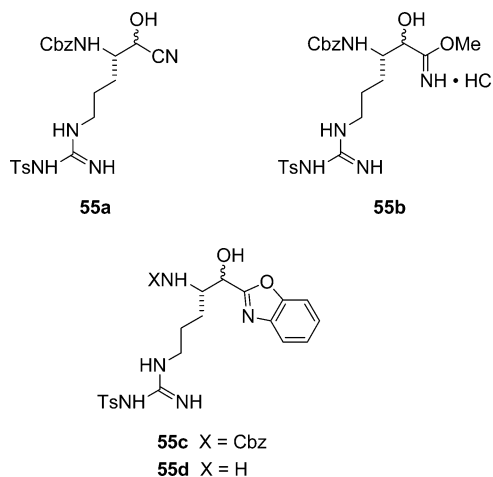
2-Aminothiophenol (2.32 g, 18.5 mmol) was added to a degassed solution of **3b** (7.23 g, 9.26 mmol) in absolute EtOH (290 mL). The resulting mixture was heated at reflux for 4.75 h, cooled to room temperature, exposed to atmospheric oxygen for 18 h, and concentrated in vacuo. The residue was purified by chromatography on silica gel, eluting with $\text{CH}_2\text{Cl}_2/\text{MeOH}$ (9:1) to provide the alcohol intermediate **3c** (3.33 g, 44%; CAS no. 178926-05-1) as a white foam.

The Dess–Martin periodinane (1.59 g, 3.76 mmol) was added to a solution of **3c** (3.08 g, 3.76 mmol) in CH_2Cl_2 (125 mL). The resulting mixture was stirred for 45 min, and an additional portion of periodinane (1.2 g, 2.83 mmol) was added, followed by another 15 min of stirring. The excess periodinane was consumed by the addition of 300 mL of quench solution (75 g of $\text{Na}_2\text{S}_2\text{O}_3$ in 300 mL of saturated aqueous NaHCO_3), diluted with EtOAc (300 mL), and vigorously stirred for 15

min. The resulting aqueous layer was isolated and extracted with EtOAc (3 \times) and the combined organic extracts were washed with successive portions of water and brine, dried (Na_2SO_4), and concentrated in vacuo to give the corresponding protected ketone (2.90 g, 94%; CAS no. 179746-19-1) as a white foam.

The protected ketone (2.97 g, 3.63 mmol) and anhydrous anisole (10 mL) were placed in a Teflon reaction tube of an HF apparatus and cooled to -78 °C. Anhydrous HF (15–20 mL) was condensed into the tube, and the temperature was increased to 0 °C. The reaction mixture was stirred at 0 °C for 2 h, concentrated in vacuo, and triturated with Et_2O (3 \times) to give a yellow solid. This solid was purified by reverse-phase HPLC, eluting with water/MeCN/TFA (70:30:0.2) to provide diastereomers **3** and **27** as glasses. Each diastereomer was dissolved in water and lyophilized to give **3** (1.11 g, 35%; slower elution) and **27** (0.10 g, 3%; faster elution) as white foams. Compound **3**: $[\alpha]_D^{20}$ -72.5° ; $^1\text{H NMR}$ δ 1.35–1.45 (m, 1H), 1.70–2.00 (m, 7H), 2.15–2.25 (m, 1H), 2.40–2.50 (m, 1H), 2.70 (s, 3H), 3.00–3.10 (m, 1H), 3.25–3.35 (m, 2H), 3.40–3.50 (m, 1H), 4.35–4.45 (m, 2H), 5.60–5.70 (m, 1H), 7.25–7.37 (ov m, 5H), 7.55–7.65 (m, 2H), 8.10 (d, 1H, $J = 6.9$ Hz), 8.20 (d, 1H, $J = 6.9$ Hz); MS (FAB) m/z 550.3 (MH)⁺. Anal. ($\text{C}_{28}\text{H}_{35}\text{N}_7\text{O}_3\text{S}\cdot 2.3\text{CF}_3\text{CO}_2\text{H}\cdot 0.8\text{H}_2\text{O}$) C, H, N, F, H₂O. Compound **27**: mp 110–120 °C; $[\alpha]_D^{20}$ -67.5° (c 0.67); IR ν_{max} 1674, 1549, 1481, 1427, 1203 cm^{-1} ; $^1\text{H NMR}$ δ 1.30–1.45 (m, 1H), 1.70–2.05 (m, 7H), 2.10–2.25 (m, 1H), 2.40–2.55 (m, 1H), 2.65 (s, 3H), 3.00–3.10 (m, 1H), 3.20–3.50 (m, 3H), 4.30–4.45 (m, 2H), 5.68–5.78 (m, 1H), 7.20–7.40 (ov m, 5H), 7.55–7.65 (m, 2H), 8.10 (d, 1H, $J = 6.9$ Hz), 8.20 (d, 1H, $J = 6.9$ Hz); MS (FAB) m/z 550.3 (MH)⁺. Anal. ($\text{C}_{28}\text{H}_{35}\text{N}_7\text{O}_3\text{S}\cdot 2.6\text{CF}_3\text{CO}_2\text{H}\cdot 1.5\text{H}_2\text{O}$) C, H, N, H₂O.

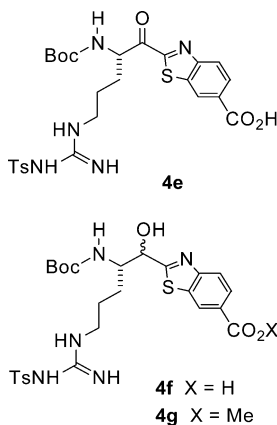
N-Methyl-D-phenylalanyl-N-[(1S)-4-[(aminoiminomethyl)amino]-1-(2-benzoxazolylcarbonyl)butyl]-L-prolinamide (55). Imidate Route Starting with an Amino Acid Aldehyde.^{21c} Anhydrous HCl gas (24 g) was bubbled into a solution of **55a**^{12b} (3.0 g, 6.3 mmol; CAS no. 186181-88-4) and



anhydrous MeOH (60 mL) at -78 °C at a rate such that the temperature did not exceed -40 °C. After the addition, the reaction mixture was stirred for 30 h at 0 °C. The reaction mixture was added to vigorously stirred saturated aqueous NaHCO_3 while maintaining the pH above 6.8. The mixture was extracted with EtOAc (100 mL), the layers were separated, and the aqueous layer was extracted with EtOAc (3 \times). The combined EtOAc extracts were washed with water (2 \times), dried (Na_2SO_4), and concentrated in vacuo to give **55b** (CAS no. 179746-31-7) as a white solid; MS (FAB) m/z 506.2 (MH)⁺. A solution of **55b** (1.00 g, 1.84 mmol), 2-aminothiophenol (0.22 g, 2.03 mmol), and absolute EtOH (40 mL) was heated at reflux under N_2 for 24 h and concentrated in vacuo. The residue was purified by normal-phase chromatography, eluting with $\text{CH}_2\text{Cl}_2/\text{MeOH}$ (95:5) to obtain **55c** as a white foam (1.04 g, 100%; CAS no. 179746-32-8); mp 81–91 °C; $[\alpha]_D^{25}$ -2.9° (c 0.68, CHCl_3). Anal. ($\text{C}_{28}\text{H}_{31}\text{N}_5\text{O}_6\text{S}\cdot 0.6\text{H}_2\text{O}$) C, H, N, H₂O.

A mixture of benzoxazole **55c** (0.87 g, 1.53 mmol), 20% Pd(OH)₂ on activated carbon (0.21 g), and absolute EtOH (19 mL) was placed on an atmospheric hydrogenator and stirred under hydrogen for 16 h. The resulting mixture was filtered through filter agent and concentrated in vacuo to give **55d** as pale-yellow foam (0.47 g, 71%; CAS no. 179746-33-9). Compound **55d** (0.47 g, 1.09 mmol) was converted to **55** according to the methods described for **4** to furnish benzoxazole **55** (0.054 g) as a white powder: mp 44–54 °C; $[\alpha]^{25}_D$ -63.3° (*c* 0.58); IR ν_{\max} 3407, 1676, 1204, 1137 cm⁻¹; ¹H NMR [(CD₃)₂CO] δ 1.35–1.45 (m, 1H), 1.07–2.00 (ov m, 8H), 2.15 (s, 2.9H), 2.25 (s, 0.1H), 2.40–2.50 (m, 1H), 3.20–3.65 (ov m, 4H), 4.40–4.50 (m, 1H), 4.50–4.60 (m, 1H), 5.45–5.55 (m, 1H), 7.30–7.40 (m, 5H), 7.55 (dd, 1H, *J* = 7.3, 7.3 Hz), 7.64 (dd, 1H, *J* = 7.3, 7.3 Hz), 7.79 (d, 1H, *J* = 7.3 Hz), 7.93 (d, 1H, *J* = 7.3 Hz); MS (FAB) *m/z* 534.3 (MH)⁺. Anal. (C₂₈H₃₅N₇O₄·0.4CF₃CO₂H·0.25H₂O) C, H, N, H₂O.

N-Methyl-D-phenylalanyl-N-[(1S)-4-[(aminoiminomethyl)amino]-1-[(6-carboxy-2-benzothiazolyl)carbonyl]butyl]-L-prolinamide (4). Weinreb Amide Route (Scheme 2). A solution of *n*-butyllithium (103 mL of 2.08 M in hexane, 214 mmol) was added dropwise to a stirred solution of benzothiazole-6-carboxylic acid (19.7 g, 111 mmol) in THF (1,386 mL) at -78 °C at a rate that kept the reaction temperature below -70 °C. On completion of addition, the dark-red reaction mixture was stirred for 34 min at -78 °C and a solution of **4a**²⁴ (4.36 g, 9.25 mmol) in THF (185 mL) was added dropwise over 15 min at a rate that maintained the reaction temperature below 70 °C. After the addition, the temperature was immediately raised to -20 °C and maintained at -24 to -20 °C for 1.5 h. The reaction was quenched with saturated aqueous NH₄Cl (790 mL), the layers were separated, and the aqueous layer was extracted with EtOAc (3×). The combined organic extracts were washed with water (2×) and brine (2×), dried (Na₂SO₄), filtered through a filter agent, and concentrated in vacuo to give crude **4e** as a solid (5.50 g, 100% yield; CAS no. 179746-75-9).



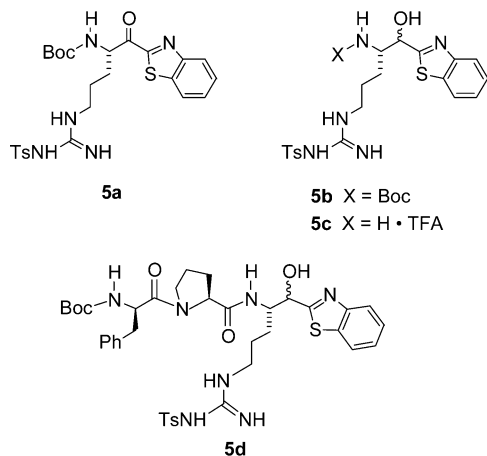
Sodium borohydride (2.12 g, 56.0 mmol) was added in one portion to a solution of the above crude acid (5.50 g, 9.34 mmol) in MeOH (140 mL) at -25 °C, and the reaction mixture was stirred at -25 to -20 °C for 1 h. The reaction was quenched by the addition of acetone (31 mL), and the mixture was stirred for 15 min and concentrated in vacuo. The residue was dissolved in water (100 mL), extracted with EtOAc (3×), and acidified to pH 3.0 with 10% aqueous citric acid. The acidic aqueous layer was extracted with EtOAc (3×) and the combined organic extracts were washed with brine (2×), dried (Na₂SO₄), and concentrated in vacuo to give crude **4f** as a light-yellow solid (4.00 g, 72%). Compound **4f** (9.70 g, 16.4 mmol) was dissolved in CH₂Cl₂/MeOH (17:3), cooled to 0 °C, and treated dropwise with (trimethylsilyl)diazomethane (2 M in hexane, 56 mL, 112 mmol) over 30 min. After 1 h, the yellow reaction mixture was concentrated in vacuo and purified by normal-phase chromatography, eluting with CH₂Cl₂/MeOH (9:1) to give **4g** as an off-white foam (2.93 g, 30%; CAS no. 186182-15-0). A solution of **4g** (2.73 g, 4.51 mmol) was

dissolved in 140 mL of TFA/CH₂Cl₂ (1:4), stirred for 2 h, and concentrated in vacuo. The residue was diluted with CH₂Cl₂ and concentrated under high vacuum to give the trifluoroacetate salt of amino alcohols **4b** (2.55 g, 91%) as a light-yellow solid. A solution of **4b** (2.55 g, 4.25 mmol) and HOBT (0.57 g, 4.25 mmol) in MeCN (196 mL) was neutralized by the addition of triethylamine (ca. 2 mL) under N₂. DCC (2.63 g, 12.8 mmol) and **4c** (0.41 g, 4.25 mmol) were added, and the reaction mixture was stirred over 18 h. The reaction mixture was filtered through filter agent, and the filtrate was concentrated in vacuo and dissolved in EtOAc. The EtOAc solution was extracted with 10% aqueous citric acid (2×), saturated aqueous NaHCO₃ (2×), and brine (2×), dried (Na₂SO₄), and concentrated in vacuo. The residue was purified by normal-phase chromatography, eluting with CH₂Cl₂/MeOH (19:1) to give the coupled product **4d** (3.05 g, 80%) as a solid.

A solution of anhydrous LiOH (1.27 g, 52.9 mmol) in water (10 mL) was added to a stirred solution of **4d** (2.26 g, 2.52 mmol) in 1,4-dioxane (100 mL) and stirred for 4 h. The resulting mixture was acidified to pH 3.0 with 10% aqueous citric acid and extracted with EtOAc (3×). The combined organic extracts were washed with brine (2×), dried (Na₂SO₄), and concentrated in vacuo. The residue (2.09 g, 2.36 mmol) was dissolved in CH₂Cl₂ (40 mL) and treated with the Dess–Martin periodinane (1.50 g, 3.53 mmol). After 2 h, the reaction mixture was treated with 100 mL of 10% aqueous Na₂S₂O₃ and stirred for 15 min. The resulting aqueous layer was isolated and extracted with CH₂Cl₂ (3×). The combined organic extracts were washed with water (2×), dried (Na₂SO₄), and concentrated in vacuo to furnish a white foam. This foam was combined with anhydrous anisole (12 mL) in a Teflon reaction tube, placed on a HF apparatus, and cooled to -78 °C. Anhydrous HF (ca. 24 mL) was condensed into the reaction tube, the temperature of the mixture was raised to 5 °C, and the mixture was stirred for 5.5 h. The reaction mixture was concentrated in vacuo and triturated three times with Et₂O (50 mL). The resulting tan solid was purified by reverse-phase HPLC, eluting with water/MeCN/TFA (90:10:0.2) to afford **4** (0.76 g, 37%) as an off-white solid: mp 110–125 °C; $[\alpha]^{25}_D$ -79.6°; IR ν_{\max} 3374, 1674, 1203 cm⁻¹; ¹H NMR δ 1.40–1.45 (m, 1H) 1.73–1.97 (m, 8H), 2.15–2.25 (m, 1H), 2.50–2.60 (m, 1H), 2.70 (s, 3H), 3.00–3.10 (m, 1H), 3.20–3.30 (m, 1H), 3.40–3.50 (m, 1H), 4.35–4.45 (m, 2H), 5.60–5.70 (m, 1H), 7.25–7.37 (ov m, 5H), 8.25 (ov s, 2H), 8.82 (s, 1H); MS (FAB) *m/z* 594.4 (MH)⁺. Anal. (C₂₉H₃₅N₇O₅S·2.5CF₃CO₂H·1.0H₂O) C, H, N, F, H₂O.

D-Phenylalanyl-N-[(1S)-4-[(aminoiminomethyl)amino]-1-(2-benzothiazolylcarbonyl)butyl]-L-prolinamide (5). A solution of butyllithium (360 mL of 0.58 M in hexane, 0.207 mol) was added dropwise over 30 min to a stirred solution of freshly distilled benzothiazole (103.1 g, 0.763 mol) in THF (2.5 L) at -78 °C under argon at a rate that kept the reaction temperature below -70 °C. Upon completion of addition, the reaction mixture was stirred for 30 min at -70 °C and a solution of **4a**²⁴ (18.0 g, 38.2 mmol; Scheme 2) in THF (1.1 L) was added dropwise over 50 min at a rate that maintained the reaction temperature below -70 °C. After the addition, the reaction mixture was stirred at -70 °C for 2 h and poured rapidly into saturated aqueous NH₄Cl (2.0 L) and vigorously stirred for 30 min. Ethyl acetate (500 mL) was added, the mixture was stirred for 15 min, and the layers were separated. The aqueous layer was extracted with EtOAc (500 mL) and the combined organic extracts were washed with water (3 × 800 mL) and brine (3 × 800 mL), dried (Na₂SO₄), filtered through filter agent, and concentrated in vacuo to afford a brown oil. This oil was partially purified by normal-phase chromatography, eluting with EtOAc/hexane (5:1) followed by trituration with hexane (4 × 500 mL) to provide **5a** as an amber glass (23.0 g, 110%).

Compound **5a** (20.8 g, 38 mmol) was dissolved in MeOH (700 mL), cooled to -20 °C, treated with sodium borohydride (4.35 g, 115 mmol), and stirred at -20 °C for 30 min. The reaction mixture was quenched by the addition of acetone (100 mL) and warmed to room temperature over 30 min. The reaction

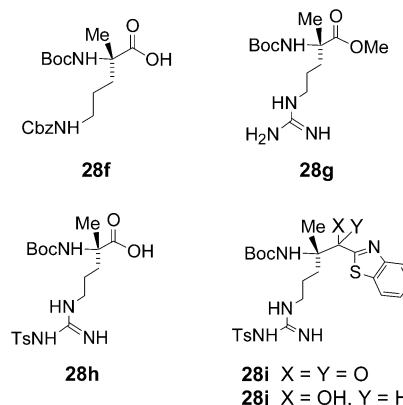


mixture was concentrated in vacuo, and the green residue was partitioned between EtOAc (300 mL) and water (150 mL). The aqueous layer was extracted with EtOAc (2 × 300 mL), and the combined organic extracts were washed with brine (2 × 50 mL), dried (Na₂SO₄), and decolorized with activated carbon. The resulting solution was filtered through filter agent and concentrated in vacuo to provide **5b** as a light-yellow solid (23 g, 110%; CAS no. 186181-82-8). Compound **5b** was added to a mixture of CH₂Cl₂ (300 mL) and TFA (75 mL). The resulting solution was stirred for 2.5 h and concentrated in vacuo. The residue was triturated with Et₂O (2 × 1 L) to furnish **5c** as a yellow solid (21.3 g, 82.6%; CAS no. 179746-24-8). A solution containing **5c** (0.796 g, 1.29 mmol), *N*-carbobenzyloxy-*D*-phenylalanyl-*L*-proline (0.509 g, 1.29 mmol), and HOBT (0.265 g, 1.96 mmol) in MeCN (25 mL) was adjusted to pH 7–8 by the addition of triethylamine (approximately 500 μL) under argon. DCC (0.404 g, 1.96 mmol) was added, and the reaction mixture was stirred over 18 h. The reaction mixture was filtered through filter agent, and the filtrate was concentrated in vacuo and dissolved in EtOAc. The EtOAc solution was extracted with 10% aqueous citric acid (2 ×), saturated aqueous NaHCO₃ (2 ×), and brine (2 ×), dried (Na₂SO₄), and concentrated in vacuo. The residue was purified by normal-phase chromatography, eluting with CH₂Cl₂/MeOH (19:1) to give **5d** (0.85 g, 80%) as a solid.

Compound **5d** (0.75 g) was oxidized with the Dess–Martin periodinane and deprotected with anhydrous HF as described for compound **4**. The resulting solid was purified by reverse-phase HPLC, eluting with water/MeCN/TFA (70:30:0.2) to give **5** (0.24 g) as a white solid: [α]_D²⁵ –79.0°; IR ν_{max} 2923, 1328, 1153, 582 cm⁻¹; ¹H NMR δ 1.50 (m, 1H), 1.70–2.05 (ov m, 7H), 2.60–2.70 (m, 1H), 3.10–3.20 (m, 2H), 3.21–3.30 (m, 2H), 3.40–3.50 (m, 1H), 4.35–4.45 (m, 2H), 5.60–5.70 (m, 1H), 7.20–7.30 (m, 2H), 7.31–7.40 (m, 3H), 7.55–7.65 (m, 2H), 8.10 (d, 1H, *J* = 6.9 Hz), 8.20 (d, 1H, *J* = 6.9 Hz); MS (FAB) *m/z* 536 (MH)⁺. Anal. (C₂₇H₃₃N₇O₇S•2.36CF₃CO₂H•0.85H₂O) C, H, N, F, H₂O.

***N*-Methyl-*D*-phenylalanyl-*N*-[(1*S*)-4-[(aminoiminomethyl)aminol]-1-(2-benzothiazolylcarbonyl)-1-methylbutyl]-*L*-prolinamide (28, Scheme 3).** A suspension of **28a**²⁷ (7.03 g, 35 mmol) in 60 mL of water was cooled to 5 °C, and the pH was adjusted to 11.0 with 3 N NaOH. Benzyl chloroformate (6.00 mL, 42 mmol) was added dropwise over 4 h while stirring at 5 °C. The reaction mixture was slowly warmed to 22 °C over 16 h and then extracted with Et₂O (3 ×). The aqueous layer was cooled to 5 °C, adjusted to pH 2.0 with 3 N HCl, and extracted with EtOAc (3 ×). The cold acidic aqueous layer was readjusted to pH 11.0 with 3 N NaOH and diluted with 175 mL of 1,4-dioxane. Di-*tert*-butyl dicarbonate (38.2 g, 175 mmol) was added in one portion at 5 °C while stirring. The reaction mixture was slowly warmed to 22 °C over 16 h, the pH was adjusted to 11.0 with 3 N NaOH, and another portion of di-*tert*-butyl dicarbonate (38.2 g, 175 mmol) was added and stirred at 22 °C over 24 h. The 1,4-dioxane was removed in vacuo, and the reaction mixture was adjusted to pH 11 with 3 N NaOH, extracted with Et₂O (3 ×), cooled to 5 °C, and

saturated with NaCl. Ethyl acetate (100 mL) was added, and the aqueous layer was adjusted to pH 4.0 with 25% aqueous citric acid (CAUTION: evolution of CO₂) while stirring at 5 °C. The layers were separated, and the acidic aqueous layer was extracted with EtOAc (5 ×). The combined EtOAc extracts were dried (MgSO₄), filtered through filter agent, and concentrated in vacuo to give **28f** (3.70 g, 56%; CAS no. 179746-65-7) as a clear glass: FAB-MS *m/z* 381 (MH)⁺.



Compound **28f** (6.86 g, 18 mmol) was dissolved in 180 mL of MeOH and combined with 20% Pd(OH)₂ on activated carbon (1.37 g) and placed under hydrogen pressure (60 psig) on a Parr hydrogenator for 18 h. The reaction mixture was filtered, and the filter cake was extracted with four 150 mL portions of hot MeOH (CAUTION). The combined MeOH extracts were filtered through filter agent and concentrated in vacuo to give **28b** (3.50 g, 79%) as a white solid: FAB-MS *m/z* 247 (MH)⁺.

Compound **28b** (3.40 g, 13.8 mmol) was combined with triethylamine (5.77 mL, 41.4 mmol) in DMF (75 mL), and to the resulting suspension was added 1,3-bis(benzyloxycarbonyl)-2-methyl-2-thiopseudourea (7.42 g, 20.7 mmol; CAS no. 25508-20-7). The resulting mixture was stirred for 1.7 days, treated with triethylamine (2.0 mL, 14.4 mmol) and 1,3-bis(benzyloxycarbonyl)-2-methyl-2-thiopseudourea (0.78 g, 2.2 mmol), stirred for 2 days, treated again with triethylamine (2.0 mL, 14.4 mmol) and 1,3-bis(benzyloxycarbonyl)-2-methyl-2-thiopseudourea (1.48 g, 4.1 mmol), and stirred at 22 °C for 3 days. The crude reaction mixture was filtered through filter agent, and the DMF was removed in vacuo. The oily residue was partitioned between 0.1 N NaOH (200 mL) and Et₂O (200 mL). The basic aqueous layer was extracted with Et₂O (4 ×), cooled to 5 °C, and adjusted to pH 3.5 with citric acid. The acidic aqueous layer was extracted with EtOAc (5 ×), and the combined EtOAc extracts were dried (Na₂SO₄), filtered through filter agent, and concentrated in vacuo. The residue was purified by normal-phase chromatography, eluting with CH₂Cl₂/MeOH (95:5) to give **28c** (5.94 g, 77%; CAS no. 179746-67-9) as a white foam: FAB-MS *m/z* 557 (MH)⁺.

A solution of **28c** (5.86 g, 10.5 mmol) in 210 mL of MeOH was treated with 20% Pd(OH)₂ on activated carbon (1.47 g), and the mixture was placed under 60 psig of hydrogen pressure on a Parr hydrogenator. After 24 h, another portion of 20% Pd(OH)₂ on activated carbon (0.74 g) was added, and the reaction was placed under 60 psig of hydrogen for 6 h. The crude reaction mixture was filtered through filter agent and concentrated in vacuo to afford **28g** (3.03 g, 100%; CAS no. 179746-68-0) as a white foam: FAB-MS *m/z* 289 (MH)⁺. Compound **28g** (0.52 g, 1.80 mmol) was dissolved in 2.7 mL of 4 N KOH, diluted with 9.0 mL of acetone, and cooled to –18 °C. To this solution was added a solution of *p*-toluenesulfonyl chloride (0.68 g, 3.60 mmol) in acetone (3.6 mL) over 15 min while stirring vigorously. After 1 h at –18 to –15 °C, the reaction was slowly warmed to 22 °C over 2.5 h. The acetone was removed in vacuo at 20 °C, and the aqueous residue was diluted with 25 mL of water and extracted with Et₂O (3 ×). The aqueous layer was saturated with NaCl, layered with EtOAc, cooled to 5 °C, and adjusted to pH 3.5 with 1 N HCl. The acidic aqueous layer was extracted with EtOAc (4 ×), and

the combined EtOAc extracts were washed with saturated aqueous NaCl (2 \times), dried (Na₂SO₄), and concentrated in vacuo to give **28h** (0.72 g, 90%; CAS no. 179746-69-1) as a white foam; FAB-MS m/z 443 (MH)⁺. Compound **28h** was dissolved in 29 mL of CH₂Cl₂/MeOH (9:1), cooled to 5 °C, and treated dropwise over 10 min with 2 M (trimethylsilyl) diazomethane in hexane (4.3 mL, 8.63 mmol). After 10 min, the reaction mixture was concentrated in vacuo at 22 °C and the residue was purified by normal-phase chromatography, eluting with EtOAc/hexane (3:2) to give **28d** (1.06 g, 81%) as a white foam; FAB-MS m/z 457 (MH)⁺.

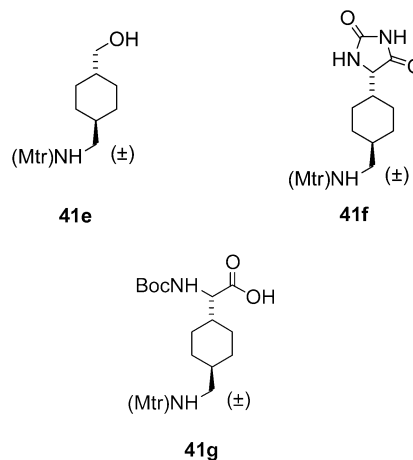
A solution of benzothiazole (2.63 g, 19.5 mmol) in 20 mL of THF was cooled to -75 °C with stirring under nitrogen. Butyllithium (1.6 M in hexane, 9.46 mL, 15.1 mmol) was added dropwise over 15 min at -75 to -65 °C and stirred for 15 min. To this solution was added dropwise over 15 min a solution of **28d** (0.46 g, 1.00 mmol) in 10 mL of THF at -75 to -70 °C. The reaction mixture was stirred at -75 °C for 2 h, and the reaction was quenched with 160 mL of saturated aqueous NH₄Cl, saturated with NaCl, and extracted with EtOAc (3 \times). The combined EtOAc extracts were washed with saturated aqueous NaCl (3 \times), dried (Na₂SO₄), and concentrated in vacuo. The residue was triturated with hexane (3 \times), dissolved in 150 mL of EtOAc/hexane (3:2), filtered through filter agent, and purified by normal-phase chromatography, eluting with EtOAc/hexane (3:2) to give 0.42 g (74%) of **28i** (0.42 g, 74%; CAS no. 179746-71-5) as clear glass: FAB-MS m/z 560 (MH)⁺. A solution of **28i** (0.40 g, 0.72 mmol) in MeOH (14 mL) was cooled to -20 °C while stirring and treated with NaBH₄ (0.081 g, 2.14 mmol). After 2.5 h, acetone (2.6 mL) was added and the reaction mixture was warmed to room temperature over 30 min. The reaction mixture was concentrated in vacuo and partitioned between water (15 mL) and EtOAc (30 mL). The aqueous layer was extracted with EtOAc (2 \times), and the combined organic extracts were washed with brine (2 \times), dried (Na₂SO₄), and concentrated in vacuo to give **28j** (0.40 g, 99%) as a tan foam. This material (0.39 g, 0.69 mmol) was dissolved in 14 mL of TFA/CH₂Cl₂ (1:4), stirred for 2 h, and concentrated in vacuo at 10 °C. The residue was partitioned between 20 mL of 1 N NaOH previously saturated with NaCl and of CH₂Cl₂ (20 mL). The basic aqueous layer was extracted with CH₂Cl₂ (3 \times), and the combined CH₂Cl₂ extracts were washed with saturated aqueous NaCl, dried (Na₂SO₄), and concentrated in vacuo to furnish **28e** (0.32 g, 100%) as a brown amorphous solid: FAB-MS m/z 462 (MH)⁺.

A solution of **4c** (0.309 g, 0.753 mmol) and diisopropylethylamine (132 μ L, 0.758 mmol) in 10 mL of anhydrous CH₂Cl₂ was cooled to 5 °C while stirring under argon. Bis(2-oxo-3-oxazolidinyl)phosphinic chloride (BOP-Cl; 0.193 g, 0.758 mmol) was added, and the reaction mixture was stirred for 15 min. A solution of **28e** (0.316 g, 0.685 mmol) and diisopropylethylamine (119 μ L, 0.684 mmol) in 10 mL of anhydrous CH₂Cl₂ was added over 10 min at 5 °C, and the reaction mixture was slowly warmed to 22 °C over 4.5 h. The reaction mixture was concentrated in vacuo at 40 °C, and the residue was partitioned between EtOAc and 1 M KHSO₄. The organic layer was extracted two more times with 1 M KHSO₄, three times with saturated aqueous NaHCO₃, and twice with saturated aqueous NaCl, dried (Na₂SO₄), and concentrated in vacuo at 40 °C. The residue was purified by normal-phase chromatography, eluting with EtOAc/hexane (4:1) to give (1*S*)-*N*-methyl-*N*-[(phenylmethoxy)carbonyl]-*D*-phenylalanyl-*N*-[1-(2-benzothiazolyl)hydroxymethyl]-4-[[imino[(4-methylphenyl)sulfonyl]amino]methyl]amino]-1-methylbutyl]-*L*-prolinamide (0.381 g, 65%; CAS no. 186182-14-9) as a white foam: FAB-MS m/z 855 (MH)⁺. This substance was converted to **28** according to the methods described for **5**. The resulting crude material was purified by reverse-phase HPLC, eluting with water/MeCN/TFA (60:40:0.2) to afford **28** as a white solid (0.094 g): mp 122–130 °C; [α]_D²⁵ -85.3° (c 0.26); IR ν_{\max} 3375, 1679, 1203 cm⁻¹; ¹H NMR δ 1.05–1.15 (m, 2H), 1.4–1.8 (ov m, 7H), 2.10–2.20 (m, 1H), 2.21–2.29 (m, 1H), 2.40–2.50 (m, 1H), 2.58 (s, 2.4H), 2.55 (s, 0.2H), 2.95–3.05 (m, 1H), 3.1–3.2 (m, 4H), 4.25–4.35 (m, 2H), 7.15–7.3 (ov m, 5H), 7.50–7.60 (m, 2H), 8.05–8.15 (m, 2H);

MS (FAB) m/z 564.3 (MH)⁺. Anal. (C₂₉H₃₇N₇O₃S₂·2.3CF₃CO₂H·1.9H₂O) C, H, N, F, H₂O: calcd 3.98; found 3.40.

(1*S*)- and (1*R*)-*N*-Methyl-*D*-phenylalanyl-*N*-[1-[[4-*trans*-(aminomethyl)cyclohexyl]methyl]-2-(2-benzothiazolyl)-2-oxoethyl]-*L*-prolinamide (**41** and **42**, Scheme 4). A slurry of **41a** (5.00 g, 31.8 mmol; CAS no. 1197-18-8; Scheme 4) in MeOH (50 mL) was treated with 4 M HCl in 1,4-dioxane, and the resulting solution was stirred for 18 h. The reaction mixture was concentrated in vacuo, dissolved in CH₂Cl₂ (50 mL), adjusted to pH 7–8 with triethylamine, and treated with 4-methoxy-2,3,6-trimethylbenzenesulfonyl chloride (7.89 g, 31.8 mmol) while cooling with a 23 °C water bath. After 4 h, the reaction mixture was filtered through filter agent and the filtrate was washed with 1 M KHSO₄ (3 \times), saturated aqueous NaHCO₃ (2 \times), and brine, dried (Na₂SO₄), filtered, and concentrated in vacuo to give **41b** (11.4 g, 94%).

A solution of **41b** (11.4 g, 29.7 mmol) in THF (150 mL) was cooled to 0 °C and treated dropwise with 1 M LiAlH₄ in THF (60 mL, 60 mmol) over 45 min. After the addition, the reaction mixture was slowly warmed to room temperature over 18 h. The reaction mixture was quenched with excess 1 N NaOH (CAUTION), filtered through filter agent, and concentrated in vacuo. The residue was dissolved in EtOAc, extracted with 1 N HCl (2 \times) and brine, dried (Na₂SO₄), filtered, and concentrated in vacuo to afford **41e** (8.09 g, 77%). A solution of **41e**



(8.09 g, 22.8 mmol) in CH₂Cl₂ (100 mL) was treated with the Dess–Martin periodinane (14.5 g, 34.1 mmol). After 2 h, 75 mL of the quench solution (25 g of Na₂S₂O₃ in 100 mL of saturated aqueous NaHCO₃) was added and the reaction mixture was stirred for 18 h. The layers were separated, and the aqueous layer was extracted with CH₂Cl₂. The combined organic extracts were washed with brine, dried (MgSO₄), and concentrated in vacuo. The residue was purified by normal-phase chromatography, eluting with hexane/EtOAc (7:3) to give **41c** (7.52 g, 93%). A slurry of **41c** (2.50 g, 7.07 mmol), ammonium carbonate (2.65 g, 27.5 mmol), and sodium cyanide (0.69 g, 10.6 mmol) in 14 mL of EtOH/water (1:1) was heated at reflux for 4 h. The reaction mixture was cooled to room temperature and acidified to pH 3 with 1 N HCl. A white precipitate formed, which was isolated by filtration and recrystallized from MeOH (1.35 g, 45%) to give **41f**. A slurry of **41f** in 4 N NaOH (25 mL) was heated at reflux for 18 h, cooled to 0 °C, and treated with di-*tert*-butyl dicarbonate (0.393 g, 1.80 mmol). The reaction mixture was slowly warmed to room temperature over 18 h, cooled to 5 °C, acidified to pH 3 with citric acid, and extracted with EtOAc (3 \times). The combined organic extracts were washed with brine, dried (Na₂SO₄), filtered, and concentrated in vacuo to furnish **41g** (0.605 g, 76%).

A solution of **41g** (0.605 g, 1.22 mmol), *N,O*-dimethylhydroxylamine·HCl (0.170 g, 1.72 mmol), and triethylamine (323 μ L, 3.32 mmol) in CH₂Cl₂ (30 mL) was treated with BOP-Cl (0.443 g, 1.74 mmol). After 4 h, the reaction mixture was quenched

with water (15 mL). The layers were separated and the organic layer was extracted with water, 10% aqueous citric acid (2×), saturated aqueous NaHCO₃ (2×), and brine, dried (MgSO₄), filtered, and concentrated in vacuo to afford **41d** (0.585, 93%). This material was converted to a mixture of **41** and **42** according to the methods described for **37** and **38**.³² The resulting crude solid was purified by reverse-phase HPLC, eluting with water/MeCN/TFA (from 80:20:0.2 to 70:30:0.2) to afford **41** (0.041 g; slower elution) and **42** (0.046 g, faster elution) as white solids. Compound **41**: ¹H NMR δ 1.05–1.15 (m, 2H), 1.35–1.45 (m, 2H), 1.60–2.00 (ov m, 8H), 2.10–2.20 (m, 2H), 2.40–2.50 (m, 1H), 2.70 (s, 3H), 2.70–2.80 (m, 2H), 3.00–3.10 (m, 1H), 3.20–3.30 (m, 1H), 3.35–3.45 (m, 1H), 4.45–3.55 (m, 2H), 5.60–5.70 (m, 1H), 7.20–7.30 (m, 2H), 7.31–7.40 (m, 3H), 7.60–7.70 (m, 2H), 8.10 (d, 1H, *J* = 7.1 Hz), 8.20 (d, 1H, *J* = 7.1 Hz); MS (ES) *m/z* 562.6 (MH)⁺. Anal. (C₃₁H₃₉N₅O₃S·2.3CF₃CO₂H·0.09HBr·1.7H₂O) C, H, N, F, Br: calcd 0.83; found 0.50. H₂O: calcd 3.55; found 2.46. Compound **42**: ¹H NMR δ 1.00–1.10 (m, 2H), 1.20–1.40 (ov m, 3H), 1.50–1.60 (m, 1H), 1.80–1.90 (m, 6H), 1.95–2.05 (m, 1H), 2.10–2.20 (m, 1H), 2.45–2.55 (m, 1H), 2.65 (s, 3H), 2.70–2.80 (m, 2H), 3.00–3.10 (m, 1H), 3.20–3.30 (m, 1H), 3.35–3.45 (m, 1H), 4.35–4.45 (m, 1H), 4.40–4.50 (m, 1H), 5.75–5.80 (m, 1H), 7.20–7.25 (m, 2H), 7.30–7.35 (m, 3H), 7.60–7.70 (m, 2H), 8.15 (d, 1H, *J* = 7.1 Hz), 8.20 (d, 1H, *J* = 7.1 Hz); MS (ES) *m/z* 562.6 (MH)⁺. Anal. C₃₁H₃₉N₅O₃S·2.27CF₃CO₂H·0.05HBr·1.6H₂O) C, H, N, Br, F, H₂O.

N-Methyl-D-phenylalanyl-N-[(1S)-1-(2-benzothiazolyl-carbonyl)-4-methoxybutyl]-L-prolinamide (43, Scheme 5). A solution of 5-methoxypentanoic acid **43b**⁶² (6.80 g, 52 mmol) and triethylamine (6.80 g, 67 mmol) in 100 mL of anhydrous THF was cooled to –78 °C while stirring under argon. Pivaloyl chloride (6.80 g, 57 mmol) was added to the reaction mixture dropwise over 15 min at –78 °C. After 15 min the reaction mixture was warmed to 0 °C, stirred for 1.5 h, and then recooled to –78 °C. Meanwhile, 1.6 M BuLi in hexane (58 mL, 93 mmol) was added dropwise to a solution of (4*S*,5*R*)-(–)-4-methyl-5-phenyl-2-oxazolidinone (16.4 g, 93 mmol) in 100 mL of THF over 30 min at –78 °C. After 15 min, this reaction mixture was added slowly to the above mixed-anhydride reaction while stirring under argon at –78 °C. The reaction mixture was slowly warmed to room temperature over 18 h, quenched with 1 N KHSO₄, and concentrated in vacuo. The residue was partitioned between water and CH₂Cl₂, and the aqueous layer was extracted with CH₂Cl₂ (3×). The combined organic extracts were washed with saturated aqueous NaCl (2×), dried (Na₂SO₄), and concentrated in vacuo. The residue was purified by normal-phase chromatography, eluting with CH₂Cl₂/EtOAc (95:5) to give **43c** (8.2 g, 55%) as a white solid: MS (FAB) *m/z* 292 (MH)⁺.

Compound **43c** (3.81 g, 13 mmol) was reacted with di-*tert*-butyl azodicarboxylate (0.48 g, 15 mmol) according to the general method of Evans et al.⁶³ The crude product was purified by normal-phase chromatography, eluting with CH₂Cl₂/hexane/MeCN (70:30:7) to give **43d** (2.33 g, 33%) as a white solid: MS (FAB) *m/z* 522 (MH)⁺.

Compound **43d** (2.33 g, 4.5 mmol) was dissolved in 18 mL of THF, cooled to 0 °C, and treated with a solution of LiOH·H₂O (0.46 g, 10.7 mmol) in 9 mL of H₂O. Aqueous H₂O₂ (1.1 mL, 30%, 10 mmol) was added, and the reaction mixture was stirred at 0 °C for 3 h. The reaction mixture was partitioned between 1 N HCl and CH₂Cl₂, and the acidic aqueous layer was extracted with CH₂Cl₂ (2×). The combined organic extracts were washed with saturated aqueous NaCl, dried (MgSO₄), and concentrated in vacuo. The residue was purified by normal-phase chromatography eluting with EtOAc/hexane/HOAc to afford **43e** (0.87 g, 56%) as a white solid: MS (FAB) *m/z* 363 (MH)⁺.

Compound **43e** (2.15 g, 5.93 mmol) was dissolved in 22 mL of TFA/CH₂Cl₂ (1:4), stirred for 1.5 h, and concentrated in vacuo. The solvents were removed in vacuo at 20 °C to furnish (S)-2-hydrazino-5-methoxypentanoic acid monotrifluoroacetate (2.07 g, >100%): MS (FAB) *m/z* 163 (MH)⁺. This material was

dissolved in absolute EtOH (100 mL), combined with PtO₂ (0.300 g), and placed on a Parr hydrogenator under hydrogen pressure (55 psig) over 24 h. The reaction mixture was filtered through filter agent and concentrated in vacuo. The residue was dissolved in MeOH (50 mL), and the pH was adjusted to pH 8 with triethylamine (ca. 2 mL). The solution was cooled to 0 °C, treated with di-*tert*-butyl dicarbonate (2.0 g, 9.0 mmol), and slowly warmed to room temperature over 20 h. The reaction mixture was concentrated in vacuo and partitioned between EtOAc (50 mL) and cold (5 °C) 1 N HCl (50 mL). The organic extract was extracted with cold 1 N HCl (50 mL), washed with saturated aqueous NaCl, dried (Na₂SO₄), and concentrated in vacuo to provide *N*-[(1,1-dimethylethoxy-carbonyl)-5-methoxy-L-norvaline (2.15 g, 68%; CAS no. 167496-30-2) as a white solid: MS (FAB) *m/z* 248 (MH)⁺. This material (1.48 g, 6.0 mmol) was combined with *N,O*-dimethylhydroxylamine hydrochloride (0.878 g, 9.0 mmol) and dissolved in 70 mL of CH₂Cl₂. The resulting mixture was adjusted to pH 8 with triethylamine and treated with BOP-Cl (2.29 g, 9.0 mmol). After 2 h, the reaction mixture was partitioned between CH₂Cl₂ and cold 1 N HCl. The organic layer was extracted with saturated aqueous NaHCO₃ and saturated aqueous NaCl, dried (MgSO₄), and concentrated in vacuo. The residue was partially dissolved in MeOH, and the insoluble material was removed by filtration. The filtrate was concentrated in vacuo to afford Weinreb amide **43f** (1.00 g, 57%) as a white solid: MS (FAB) *m/z* 291 (MH)⁺. Weinreb amide **43f** (0.87 g, 3.0 mmol) was converted to **43** according to the methods described for **5**. The resulting crude product was purified by reverse-phase HPLC, eluting with water/MeCN/TFA (50:50:0.2) to afford **43** (0.120 g) as a white solid: [α]_D²⁵ –18.0°; IR ν_{max} 3430, 2929, 1677, 1204 cm⁻¹; ¹H NMR (CDCl₃) δ 1.35–1.45 (m, 1H), 1.70–2.00 (ov m, 2H), 2.15–2.25 (m, 2H), 2.40–2.50 (m, 1H), 2.65 (s, 3H), 2.95–3.05 (m, 1H), 3.30 (s, 3H), 3.40–3.50 (m, 3H), 4.30–4.40 (m, 2H), 5.60–5.65 (m, 0.8H), 5.65–5.70 (m, 0.2H), 7.20–7.29 (m, 2H), 7.30–7.35 (m, 3H), 7.55–7.65 (m, 2H), 8.10 (d, 1H, *J* = 7.1 Hz), 8.20 (d, 1H, *J* = 7.1 Hz); MS (FAB) *m/z* 523.4 (MH)⁺. Anal. (C₂₈H₃₄N₄O₄S·1.5CF₃CO₂H·1.1H₂O) C, H, N, F, H₂O.

N-Methyl-D-phenylalanyl-N-[1-*trans*-4-aminocyclohexyl]-3-(2-benzothiazolyl)-3-oxopropyl]-L-prolinamide (71 and 72, Scheme 6). A slurry of **69d**³² (4.41 g, 13.0 mmol), ammonium acetate (1.50 g, 19.5 mmol), and malonic acid (1.35 g, 13.0 mmol) in absolute EtOH (25 mL) was heated at reflux for 18 h. The reaction mixture was cooled to room temperature and diluted with water (25 mL). The resulting precipitate was collected and dried in vacuo to give **71a** (2.95 g, 57%) as a white solid. This material (2.95 g, 7.4 mmol) was dissolved in MeOH (70 mL), basified with triethylamine (3.1 mL, 22 mmol), and treated with di-*tert*-butyl dicarbonate (1.80 g, 8.30 mmol) while stirring. After 18 h, the reaction mixture was dissolved in EtOAc and extracted with 1 M KHSO₄ (2×) and brine, dried (Na₂SO₄), filtered, and concentrated in vacuo. The residue was purified by normal-phase chromatography, eluting with CH₂Cl₂/MeOH (19:1) to give the corresponding Boc-protected product (0.635 g, 17%). This material (0.24 g, 0.48 mmol) was converted to Weinreb amide **71d** as described for **41**. Compound **71b** (0.10 g, 0.18 mmol) was converted to a 1:1 mixture of **71** and **72** according to the methods used for **41**. The resulting crude solid was purified by reverse-phase HPLC, eluting with water/MeCN/TFA (from 90:10:0.2 to 60:40:0.2) to afford **71** (0.015 g, slower elution) and **72** (0.015 g, faster elution) as white solids. Compound **71**: HPLC purity = 97%; ¹H NMR δ 1.15–2.30 (ov m, 16H), 2.80–3.20 (ov m, 6H), 3.55–3.73 (ov m, 1H), 4.25–4.45 (ov m, 2H), 5.60–5.70 (ov m, 1H), 7.20–7.35 (m, 5H), 8.10–8.25 (ov m, 2H); MS (ES) *m/z* 562.3 (MH)⁺; HRMS *m/z* 562.2852 (562.2852 calcd for C₃₁H₃₉N₅O₃S + H⁺). Compound **72**: HPLC purity = 99%; ¹H NMR δ 1.27–1.43 (ov m, 5H), 1.65–1.77 (ov m, 4H), 2.03–2.13 (ov m, 4H), 2.40–2.45 (m, 1H), 2.64 (s, 3H), 3.01–3.40 (m, 5H), 3.60–3.65 (m, 1H), 4.10–4.18 (m, 1H), 4.30–4.35 (m, 2H), 7.20–7.26 (m, 2H), 7.30–7.35 (m, 3H), 7.57–7.65 (m, 2H), 8.08 (d, 1H, *J* = 7.65 Hz), 8.18 (d, 1H, *J* = 7.65 Hz); MS (ES) *m/z* 562.3 (MH)⁺; HRMS *m/z* 562.2873 (562.2852 calcd for C₃₁H₃₉N₅O₃S + H⁺).

Thrombin Inhibition Assay.³² Thrombin-catalyzed hydrolysis rates were measured spectrophotometrically using commercial human α -thrombin (American Diagnostica), a chromogenic substrate (Spectrozyme TH (H-D-HHT-Ala-Arg-pNA \cdot 2AcOH), American Diagnostica) in aqueous buffer (10 mM Tris, 10 mM Hepes, 150 mM NaCl, 0.1% PEG; pH 7.4), and a microplate reader (Molecular Devices). Changes in absorbance at 405 nm were monitored (Softmax, Molecular Devices) upon addition of enzyme both with and without inhibitor present at 37 °C over 30 min. The IC₅₀ values were determined by fixing the enzyme and substrate concentrations and varying the inhibitor concentration (1 nM thrombin, 50 μ M Spectrozyme TH). Michaelis–Menton kinetics were applied to the initial reaction slopes. Inhibition constants (K_i) were determined by fixing the enzyme and inhibitor concentrations and varying the substrate concentration (1 nM thrombin, 5–100 μ M Spectrozyme TH). Michaelis–Menton kinetics were applied to the initial reaction slopes using the program K-Cat (Bio Metallics Inc.).

Trypsin Inhibition Assay.³² Trypsin-catalyzed hydrolysis rates were measured using the same method as the thrombin procedure. Bovine type 1 trypsin (Sigma) and Spectrozyme TRY (Cbo-Gly-D-Ala-Arg-pNA \cdot AcOH, American Diagnostics) replaced their thrombin equivalents in a concentration range of 3.2 U/mL trypsin and 0.1–0.3 mM Spectrozyme.

Gel-Filtered Platelet Aggregation. Gel-filtered platelet preparations allow assessment of antiplatelet activity in the absence of plasma coagulation factors and fibrinogen. α -Thrombin, which induces platelet aggregation and fibrin clot formation, can only be tested in such a preparation. Human platelet-rich plasma (PRP) concentrate was gel-filtered on a Sepharose 2B column with Tyrode's buffer (140 mM NaCl, 2.7 mM KCl, 12 mM NaHCO₃, 0.76 mM Na₂HPO₄, 5.5 mM glucose, 5.0 mM Hepes, and 2 mg/mL BSA; pH 7.4). The gel-filtered platelets were diluted with Tyrode's buffer, compound solution in buffer, and 2 mM CaCl₂ to achieve ca. 142 900 platelets/ μ L final assay concentration on the 96-well assay plates. Platelet aggregation was initiated by the addition of a concentration of human α -thrombin shown in preliminary experiments (on the day of the test) to achieve 80% aggregation (0.005–0.25 NIH U/mL). The assay plate was stirred and intermittently placed in a microplate reader to read optical density (650 nm) at 0 and 7 min after the thrombin addition. Aggregation was calculated to be the decrease in optical density between the time zero and 7 min measurements. The assay was determined to be valid when the percent aggregation of the control is >75%. Each concentration of compounds, vehicles, and buffer controls were run in duplicate. Inhibition was calculated by comparing to wells containing no inhibitor (vehicle), and IC₅₀ values were determined using a four-parameter fit logistics model.

Acknowledgment. We thank Dr. Lisa Minor and Yuanping Wang for several enzymatic studies, Michael Addo for the platelet aggregation studies, George Greco for some synthetic intermediates, and Michael Moyer and Rekha Shah for epimerization studies and analytical HPLC assays. We are grateful to Dr. Michael Greco and Dr. Enrico Di Cera (Washington University) for helpful discussions and advice.

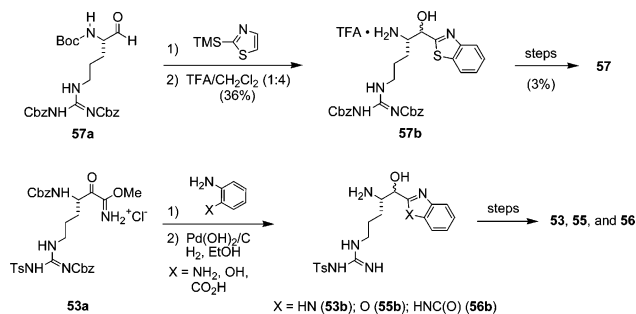
Supporting Information Available: Table 7, experimental procedures and characterization data for **6–20**, **22**, **24–26**, **29–40**, **44–54**, **56–70**, and **73–77** (with associated refs 57–61 and 64–70), stereochemical stability profile of **3** in rabbit and rat plasma, enzyme inhibition assay procedures, K_i values for Table 9, in vivo assay procedures, and microanalytical data. This material is available free of charge via the Internet at <http://pubs.acs.org>.

References

- (1) (a) This paper is dedicated to the memory of Dr. Paul A. J. Janssen, one of the most prolific pharmaceutical researchers of all time. (b) This work was presented in part at the 216th National Meeting of the American Chemical Society, Boston, MA, August 1998; Abstract MEDI-021.
- (2) Reviews pertinent to structure-based drug design and discovery: (a) Appelt, K. Bacquet, R. J.; Bartlett, C. A.; Booth, C. L.; Freer, S. T.; Fuhry, M. A.; Gehring, M. R.; Herrmann, S. M.; Howland, E. F.; Janson, C. A.; et al. Design of enzyme inhibitors using iterative protein crystallographic analysis. *J. Med. Chem.* **1991**, *34*, 1925–1934. (b) Greer, J.; Erickson, J. W.; Baldwin, J. J.; Varney, M. D. Application of the three-dimensional structures of protein target molecules in structure-based drug design. *J. Med. Chem.* **1994**, *37*, 1035–1054. (c) Reickson, J. W.; Fesik, S. W. Macromolecular X-ray crystallography and NMR as tools for structure-based drug design. *Annu. Rev. Med. Chem.* **1992**, *27*, 217–289. (d) McDowell, R. S.; Artis, D. R. Structure-based design from flexible ligands. *J. Med. Chem.* **1995**, *30*, 265–274. (e) Kuntz, I. D.; Meng, E. C.; Shoichet, B. K. Structure-based molecular design. *Acc. Chem. Res.* **1994**, *27*, 117–123. (f) Bode, W.; Huber, R. Structural basis of the endoprotease–protein inhibitor interaction. *Biochim. Biophys. Acta* **2000**, *1477*, 241–252.
- (3) (a) α -Thrombin is a member of the trypsin-like serine protease family. The catalytic machinery in the active site of thrombin and other serine proteases is comprised of the catalytic triad His-57, Asp-104, and Ser-195 (chymotrypsinogen numbering system^{4a}). (b) Throughout this paper, the term “thrombin” refers to “ α -thrombin”.
- (4) (a) Bode, W.; Mayr, I.; Baumann, U.; Huber, R.; Stone, S. R.; Hofsteenge, J. The refined 1.9 Å crystal structure of α -thrombin: interaction with D-Phe-Pro-Arg chloromethylketone and significance of the Tyr-Pro-Pro-Trp insertion segment. *EMBO J.* **1989**, *8*, 3467–3475. (b) Bode, W.; Turk, D.; Karshikov, A. The refined 1.9 Å X-ray crystal structure of D-Phe-Pro-Arg chloromethylketone-inhibited human α -thrombin: structure analysis, overall structure, electrostatic properties, detailed active-site geometry, and structure–function relationships. *Protein Sci.* **1992**, *1*, 426–471.
- (5) (a) Berliner, L. J., Ed. *Thrombin: Structure and Function*; Plenum Press: New York, 1992. (b) Davie, E. W.; Fugikawa, K.; Kisiel, W. The coagulation cascade: initiation, maintenance, and regulation. *Biochemistry* **1991**, *30*, 10363–10370.
- (6) For reviews on thrombin inhibitors, see the following: (a) Maffrand, J. P. Direct thrombin inhibitors. *Nouv. Rev. Fr. Hematol.* **1992**, *34*, 405–419. (b) Talbot, M. D.; Butler, K. D. Potential clinical uses of thrombin inhibitors. *Drug News Perspect.* **1990**, *3*, 357–363. (c) Das, J.; Kimball, S. D. Thrombin active site inhibitors. *Bioorg. Med. Chem.* **1995**, *3*, 999–1007. (d) Scarborough, R. M. Anticoagulant strategies targeting thrombin and factor Xa. *Annu. Rev. Med. Chem.* **1995**, *30*, 71–80. (e) Kimball, S. D. Thrombin active site inhibitors. *Curr. Pharm. Des.* **1995**, *1*, 441–468. (f) Fareed, J.; Callas, D. D. Pharmacological aspects of thrombin inhibitors: a developmental perspective. *Vessels* **1995**, *1*, 15–24. (g) Lefkowitz, J.; Topol, E. J. Direct thrombin inhibitors in cardiovascular medicine. *Circulation* **1994**, *90*, 1522–1536. (h) Betschmann, P.; Lerner, C.; Sahli, S.; Obst, U.; Diederich, F. Molecular recognition with biological receptors: structure-based design of thrombin inhibitors. *Chimia* **2000**, *54*, 633–639. (i) Menear, K. Direct thrombin inhibitors: Current status and future prospects. *Expert Opin. Invest. Drugs* **1999**, *8*, 1373–1384. (j) Ripka, W. C.; Vlasuk, G. P. Antithrombotics/serine proteases. *Annu. Rev. Med. Chem.* **1997**, *32*, 71–89. (k) Sanderson, P. E. J. Small, noncovalent serine protease inhibitors. *Med. Res. Rev.* **1999**, *19*, 179–197. (l) Kimball, S. D. Challenges in the development of orally bioavailable thrombin active site inhibitors. *Blood Coagulation Fibrinolysis* **1995**, *6*, 511–519.
- (7) (a) Kettner, C.; Shaw, E. D-Phe-Pro-ArgCH₂Cl—a selective affinity label for thrombin. *Thromb. Res.* **1979**, *14*, 969–973. (b) Hauptmann, J.; Markwardt, F. Studies on the anticoagulant and antithrombotic action of an irreversible thrombin inhibitor. *Thromb. Res.* **1980**, *20*, 347–351.
- (8) (a) Please note that the term “transition-state analogue” is used somewhat loosely in this paper. “Reaction coordinate analogue” has been proposed as a more precise term for a reversible enzyme inhibitor involving an electrophilic center that covalently attaches to a group in the enzyme active site.^{8b} (b) Christianson, D. W.; Lipscomb, W. N. Carboxypeptidase A. *Acc. Chem. Res.* **1989**, *22*, 62–69.
- (9) For ease of discussion, Schechter and Berger's nomenclature system designating the amino acid residues flanking the scissile bond is used throughout this paper. Schechter, I.; Berger, A. On the size of the active site in proteases. I. Papain. *Biochem. Biophys. Res. Commun.* **1967**, *27*, 157–162.
- (10) Rydel, T. J.; Ravichandran, K. G.; Tulinsky, A.; Bode, W.; Huber, R.; Roitsch, C.; Fenton, J. W., II. The structure of a complex of recombinant hirudin and human α -thrombin. *Science* **1990**, *249*, 277–280.
- (11) (a) Bajusz, S.; Széll, E.; Bagdy, D.; Barabás, E.; Horvath, G.; Dioszegi, M.; Fittler, Z.; Szabo, G.; Juhász, A.; Tomori, E.; Szilagy, G. Highly active and selective anticoagulants: D-Phe-Pro-Arg-H, a free tripeptide aldehyde prone to spontaneous

- inactivation, and its stable *N*-methyl derivative, *D*-MePhe-Pro-Arg-H. *J. Med. Chem.* **1990**, *33*, 1729–1735. (b) Tomori, É.; Széll, E.; Barabás, É. High-performance liquid chromatography of a new tripeptide aldehyde (GYKI-14166), correlation between the structure and activity. *Chromatographia* **1984**, *437*–442. (c) Bajusz, S.; Barabás, E.; Fauszt, I.; Feher, A.; Horvath, G.; Juhasz, A.; Szabo, A. G.; Széll, E. Active site-directed thrombin inhibitors: α -hydroxyacyl-prolyl-arginals. New orally active stable analogs of *D*-Phe-Pro-Arg-H. *Bioorg. Med. Chem.* **1995**, *3*, 1079–1089. (d) Shuman, R. T.; Rothenberger, R. B.; Campbell, C. S.; Smith, G. F.; Gifford-Moore, D. S.; Gesellchen, P. D. Highly selective tripeptide thrombin inhibitors. *J. Med. Chem.* **1993**, *36*, 314–319.
- (12) (a) Maryanoff, B. E.; Qiu, X.; Padmanabhan, K. P.; Tulinsky, A.; Almond, H. R., Jr.; Andrade-Gordon, P.; Greco, M. N.; Kauffman, J. A.; Nicolaou, K. C.; Liu, A.; Brungs, P. H.; Fusetani, N. Molecular basis for the inhibition of human α -thrombin by the macrocyclic peptide cyclotheonamide A. *Proc. Natl. Acad. Sci. U.S.A.* **1993**, *90*, 8048–8052. (b) Maryanoff, B. E.; Greco, M. N.; Zhang, H.-C.; Andrade-Gordon, P.; Kauffman, J. A.; Nicolaou, K. C.; Liu, A.; Brungs, P. H. Macrocyclic peptide inhibitors of serine proteases. Convergent synthesis of cyclotheonamides A and B via a late-stage primary amine intermediate. Study of thrombin inhibition under diverse conditions. *J. Am. Chem. Soc.* **1995**, *117*, 1225–1239.
- (13) Maryanoff, B. E.; Zhang, H.-C.; Greco, M. N.; Glover, K. A.; Kauffman, J. A.; Andrade-Gordon, P. Cyclotheonamide derivatives: synthesis and thrombin inhibition. Exploration of specific structure–function issues. *Bioorg. Med. Chem.* **1995**, *3*, 1025–1038.
- (14) Costanzo, M. J.; Maryanoff, B. E.; Hecker, L. R.; Schott, M. R.; Yabut, S. C.; Zhang, H.-C.; Andrade-Gordon, P.; Kauffman, J. A.; Lewis, J. M.; Krishnan, R.; Tulinsky, A. Potent thrombin inhibitors that probe the S₁' subsite: tripeptide transition state analogs based on a heterocycle-activated carbonyl group. *J. Med. Chem.* **1996**, *39*, 3039–3043.
- (15) (a) Matthews, J. H.; Krishnan, R.; Costanzo, M. J.; Maryanoff, B. E.; Tulinsky, A. Crystal structures of thrombin with thiazole-containing inhibitors: probes of the S₁' binding site. *Biophys. J.* **1996**, *71*, 2830–2839. (b) Recacha, R.; Costanzo, M. J.; Maryanoff, B. E.; Carson, M.; DeLucas, L. J.; Chattopadhyay, D. Crystal structure of human α -thrombin complexed with RWJ-51438 at 1.7 Å: unusual perturbation of the 60A–60I insertion loop. *Acta Crystallogr., Sect. D: Biol. Crystallogr.* **2000**, *56*, 1395–1400.
- (16) Giardino, E. C.; Costanzo, M. J.; Kauffman, J. A.; Li, Q. S.; Maryanoff, B. E.; Andrade-Gordon, P. Antithrombotic properties of RWJ-50353, a potent and novel thrombin inhibitor. *Thromb. Res.* **2000**, *98*, 83–93.
- (17) Ketoheterocycle elastase inhibitors: (a) Edwards, P. D.; Meyer, E. F., Jr.; Vijayalakshmi, J.; Tuthill, P. A.; Andisik, D. A.; Gomes, B.; Strimpler, A. Design, synthesis, and kinetic evaluation of a unique class of elastase inhibitors, the peptidyl α -ketobenzoxazoles, and the X-ray crystal structure of the covalent complex between porcine pancreatic elastase and Ac-Ala-Pro-Val-2-benzoxazole. *J. Am. Chem. Soc.* **1992**, *114*, 1854–1863. (b) Edwards, P. D.; Wolanin, D. J.; Andisik, D. W.; Davis, M. W. Peptidyl α -ketoheterocyclic inhibitors of human neutrophil elastase. 2. Effect of varying the heterocyclic ring on in vitro potency. *J. Med. Chem.* **1995**, *38*, 76–85. (c) Edwards, P. D.; Zottola, M. A.; Davis, M. W.; Williams, J.; Tuthill, P. A. Peptidyl α -ketoheterocyclic inhibitors of human neutrophil elastase. 3. In vitro and in vivo potency of a series of peptidyl α -ketobenzoxazoles. *J. Med. Chem.* **1995**, *38*, 3972–3982.
- (18) Ketoheterocycle thrombin inhibitors published after ref 14: (a) Akiyama, Y.; Tsutsumi, S.; Hatsushiba, E.; Ohuchi, S.; Okonogi, T. Peptidyl α -keto thiazole as potent thrombin inhibitors. *Bioorg. Med. Chem. Lett.* **1997**, *7*, 533–538. (b) Tamura, S. Y.; Shamblyn, B. M.; Brunck, T. K.; Ripka, W. C. Rational design, synthesis and serine protease inhibitory activity of novel P₁-argininoyl heterocycles. *Bioorg. Med. Chem. Lett.* **1997**, *7*, 1359–1364. (c) Boatman, P. D.; Ogbu, C. O.; Eguchi, M.; Kim, H.-O.; Nakanishi, H.; Cao, B.; Shea, J. P.; Kahn, M. Secondary structure peptide mimetics: design, synthesis, and evaluation of β -strand mimetic thrombin inhibitors. *J. Med. Chem.* **1999**, *42*, 1367–1375. (d) St. Denis, Y.; Augelli-Szafran, C. E.; Bachand, B.; Berryman, K. A.; DiMaio, J.; Doherty, A. M.; Edmunds, J. J.; Leblond, L.; Levesque, S.; Narasimhan, L. S.; Penvose-Yi, J. R.; Rubin, J. R.; Tarazi, M.; Winocour, P. D.; Siddiqui, M. A. Potent bicyclic lactam inhibitors of thrombin: Part I: P₃ modifications. *Bioorg. Med. Chem. Lett.* **1998**, *8*, 3193–3198. (e) Plummer, J. S.; Berryman, K. A.; Cai, C.; Cody, W. L.; DiMaio, J.; Doherty, A. M.; Edmunds, J. J.; He, J. X.; Holland, D. R.; Levesque, S.; Kent, D. R.; Narasimhan, L. S.; Rubin, J. R.; Rapundalo, S. T.; Siddiqui, M. A.; Susser, A. J.; St. Denis, Y.; Winocour, P. D. Potent and selective bicyclic lactam inhibitors of thrombin: part 2: P₁ modifications. *Bioorg. Med. Chem. Lett.* **1998**, *8*, 3409–3414. (f) Plummer, J. S.; Berryman, K. A.; Cai, C.; Cody, W. L.; DiMaio, J.; Doherty, A. M.; Eaton, S.; Edmunds, J. J.; Holland, D. R.; Lafleur, D.; Levesque, S.; Narasimhan, L. S.; Rubin, J. R.; Rapundalo, S. T.; Siddiqui, M. A.; Susser, A.; St. Denis, Y.; Winocour, P. D. Potent and selective bicyclic lactam inhibitors of thrombin: Part 3: P₁' modifications. *Bioorg. Med. Chem. Lett.* **1999**, *9*, 835–840. (g) Leblond, L.; Grouix, B.; Boudreau, C.; Yang, Q.; Siddiqui, M. A.; Winocour, P. D. In vitro and in vivo properties of bicyclic lactam inhibitors. A novel class of low molecular weight peptidomimetic thrombin inhibitors. *Thromb. Res.* **2000**, *100*, 195–209. (h) Narasimhan, L. S.; Rubin, J. R.; Holland, D. R.; Plummer, J. S.; Rapundalo, S. T.; Edmunds, J. E.; St. Denis, Y.; Siddiqui, M. A.; Humblet, C. Structural basis of the thrombin selectivity of a ligand that contains the constrained arginine mimic (2*S*)-2-amino-(3*S*)-3-(1-carbamimidoyl-piperidin-3-yl)-propanoic acid at P₁. *J. Med. Chem.* **2000**, *43*, 361–368. (i) Bachand, B.; Tarazi, M.; St. Denis, Y.; Edmunds, J. J.; Winocour, P. D.; Leblond, L.; Siddiqui, M. A. Potent and selective bicyclic lactam inhibitors of thrombin. Part 4: transition state inhibitors. *Bioorg. Med. Chem. Lett.* **2001**, *11*, 287–290. (j) Cody, W. L.; Cai, C.; Doherty, A. M.; Edmunds, J. J.; He, J. X.; Narasimhan, L. S.; Plummer, J. S.; Rapundalo, S. T.; Rubin, J. R.; Van Huis, C. A.; St. Denis, Y.; Winocour, P. D.; Siddiqui, M. A. The design of potent and selective inhibitors of thrombin utilizing a piperazinedione template. Part 1. *Bioorg. Med. Chem. Lett.* **1999**, *9*, 2497–2502. (k) Cody, W. L.; Augelli-Szafran, C. E.; Berryman, K. A.; Cai, C.; Doherty, A. M.; Edmunds, J. J.; He, J. X.; Narasimhan, L. S.; Penvose-Yi, J.; Plummer, J. S.; Rapundalo, S. T.; Rubin, J. R.; Van Huis, C. A.; Leblond, L.; Winocour, P. D.; Siddiqui, M. A. The design of potent and selective inhibitors of thrombin utilizing a piperazinedione template: part 2. *Bioorg. Med. Chem. Lett.* **1999**, *9*, 2503–2508. (l) Adang, A. E. P.; de Man, A. P. A.; Vogel, G. M. T.; Grootenhuis, P. D. J.; Smit, M. J.; Peters, C. A. M.; Visser, A.; Rewinkel, J. B. M.; van Dinther, T.; Lucas, H.; Kelder, J.; van Aelst, S.; Meuleman, D. G.; van Boeckel, C. A. A. Unique overlap in the prerequisites for thrombin inhibition and oral bioavailability resulting in potent oral antithrombotics. *J. Med. Chem.* **2002**, *45*, 4419–4432.
- (19) Ketoheterocycle inhibitors of serine proteases other than elastase and thrombin: (a) Tsutsumi, S.; Okonogi, T.; Shibahara, S.; Patchett, A. A.; Christensen, B. G. α -Ketothiazole inhibitors of prolyl endopeptidase. *Bioorg. Med. Chem. Lett.* **1994**, *4*, 831–834. (b) Tsutsumi, S.; Okonogi, T.; Shibahara, S.; Ohuchi, S.; Hatsushiba, E.; Patchett, A. A.; Christensen, B. G. Synthesis and structure–activity relationships of peptidyl α -keto heterocycles as novel inhibitors of prolyl endopeptidase. *J. Med. Chem.* **1994**, *37*, 3492–3502. (c) Ogilvie, W.; Bailey, M.; Poupard, M.-A.; Abraham, A.; Bhavsar, A.; Bonneau, P.; Bordeleau, J.; Bousquet, Y.; Chabot, C.; Duceppe, J.-S.; Fazel, G.; Goulet, S.; Grand-Maitre, C.; Guse, I.; Halmos, T.; Lavallee, P.; Leach, M.; Malenfant, E.; O'Meara, J.; Plante, R.; Plouffe, P.; Poirier, M.; Soucy, F.; Yoakim, C.; Deziel, R. Peptidomimetic inhibitors of the human cytomegalovirus protease. *J. Med. Chem.* **1997**, *40*, 4113–4135. (d) Boger, D. L.; Miyauchi, H.; Hedrick, M. P. α -Keto heterocycle inhibitors of fatty acid amide hydrolase: Carbonyl group modification and α -substitution. *Bioorg. Med. Chem. Lett.* **2001**, *11*, 1517–1520. (e) Zhu, B. Y.; Huang, W.; Su, T.; Marlowe, C.; Sinha, U.; Hollenbach, S.; Scarborough, R. M. Discovery of transition state factor Xa inhibitors as potential anticoagulant agents. *Curr. Top. Med. Chem.* **2001**, *1*, 101–119. (f) Akahoshi, F.; Ashimori, A.; Sakashita, H.; Yoshimura, T.; Imada, T.; Nakajima, M.; Mitsutomi, N.; Kuwahara, S.; Ohtsuka, T.; Fukaya, C.; Miyazaki, M.; Nakamura, N. Synthesis, structure–activity relationships, and pharmacokinetic profiles of nonpeptidic α -keto heterocycles as novel inhibitors of human chymase. *J. Med. Chem.* **2001**, *44*, 1286–1296. (g) Narjes, F.; Koehler, K. F.; Koch, U.; Gerlach, B.; Colarusso, S.; Steinkuhler, C.; Brunetti, M.; Altamura, S.; De Francesco, R.; Matassa, V. G. A designed P₁ cysteine mimetic for covalent and noncovalent inhibitors of HCV NS3 protease. *Bioorg. Med. Chem. Lett.* **2002**, *12*, 701–704. (h) South, M. S.; Case, B. L.; Wood, R. S.; Jones, D. E.; Hayes, M. J.; Girard, T. J.; Lachance, R. M.; Nicholson, N. S.; Clare, M.; Stevens, A. M.; Stegeman, R. A.; Stallings, W. C.; Kurumbail, R. G.; Parlow, J. J. Structure-based drug design of pyrazinone antithrombotics as selective inhibitors of the tissue factor VIIa complex. *Bioorg. Med. Chem. Lett.* **2003**, *13*, 2319–2325. (i) Akahoshi, F. Nonpeptidic chymase inhibitors: design and structure–activity relationships of pyrimidinone derivatives based on the predicted binding mode of a peptidic inhibitor. *Curr. Pharm. Des.* **2003**, *9*, 1191–1199. (j) Costanzo, M. J.; Yabut, S. C.; Almond, H. R., Jr.; Andrade-Gordon, P.; Corcoran, T. W.; de Garavilla, L.; Kauffman, J. A.; Abraham, W. M.; Recacha, R.; Chattopadhyay, D.; Maryanoff, B. E. Potent, small-molecule inhibitors of human mast cell tryptase. Anti-asthmatic action of a dipeptide-based transition-state analogue containing a benzothiazole ketone. *J. Med. Chem.* **2003**, *46*, 3865–3876.

- (20) Ketoheterocycle cysteine protease inhibitors: (a) Tao, M.; Bihovsky, R.; Kauer, J. C. Inhibition of calpain by peptidyl heterocycles. *Bioorg. Med. Chem. Lett.* **1996**, *6*, 3009–3012. (b) Dragovich, P. S.; Zhou, R.; Webber, S. E.; Prins, T. J.; Kwok, A. K.; Okano, K.; Fuhrman, S. A.; Zalman, L. S.; Maldonado, F. C.; Brown, E. L.; et al. Structure-based design of ketone-containing, tripeptidyl human rhinovirus 3C protease inhibitors. *Bioorg. Med. Chem. Lett.* **2000**, *10*, 45–48.
- (21) (a) We prepared **4–52**, **54**, and **61–76** from the appropriate lithio heterocycles by using the methods outlined for **3** in Scheme 2. (b) Preparation of **57**: Aldehyde **57a** was reacted with 2-(trimethylsilyl)thiazole²² and deprotected with TFA to give **57b**, which was converted to **57** by the method used for **4b** in Scheme 2. (c) Preparation of **53**, **55**, and **56**: Imidate **53a**^{11b} was reacted with 2-aminophenol, *o*-phenylenediamine, or anthranilic acid, followed by hydrogenolysis, to afford **53b**, **55b**, and **56b**, respectively. These compounds were then converted to their targets by the method described for **4b** in Scheme 2. This route was generally more applicable than the tripeptidyl imidate route (Scheme 1).



- (22) Dondoni, A.; Perrone, D.; Merino, P. Chelation- and nonchelation-controlled addition of 2-(trimethylsilyl)thiazole to α -amino aldehydes: stereoselective synthesis of the β -amino- α -hydroxy aldehyde intermediate for the preparation of the human immunodeficiency virus proteinase inhibitor Ro 31-8959. *J. Org. Chem.* **1995**, *60*, 8074–8080.
- (23) Dess, D. B.; Martin, J. C. A useful 12-I-5 triacetoxyperiodinane (the Dess–Martin periodinane) for the selective oxidation of primary or secondary alcohols and a variety of related 12-I-5 species. *J. Am. Chem. Soc.* **1991**, *113*, 7277–7287.
- (24) DiMaio, J.; Gibbs, B.; Lefebvre, J.; Konishi, Y.; Munn, D.; Yue, S. Y. Synthesis of a homologous series of ketomethylene arginyl pseudopeptides and application to low molecular weight hirudin-like thrombin inhibitors. *J. Med. Chem.* **1992**, *35*, 3331–3341.
- (25) Reetz, M. T.; Drewes, M. W.; Lennick, K.; Schmitz, A.; Holdgrün, X. Nonracemizing synthesis and stereoselective reduction of chiral α -amino ketones. *Tetrahedron: Asymmetry* **1990**, *1*, 375–378.
- (26) The identity of **27**, the D-epimer of **3**, was confirmed by independent synthesis. The identities of compounds **3**, **4**, and **23** were confirmed by X-ray crystal structures. The identities of the remaining compounds (**5–20**, **24–26**, **28–77**) were assigned by both elution order (D-epimer elutes before L-epimer) and thrombin affinity (L-epimer has higher thrombin and trypsin affinities).
- (27) Tian, Z.; Edwards, P.; Roeske, R. W. Synthesis of optically pure C⁶-methyl-arginine. *Int. J. Pept. Protein Res.* **1992**, *40*, 119–126.
- (28) Abbreviations: BOP-Cl, bis(2-oxo-3-oxazolidinyl)phosphinic chloride; BOP, benzotriazol-1-yloxytris(dimethylamino)phosphonium hexafluorophosphate; PyBrOP, bromotris(pyrrolidino)phosphonium hexafluorophosphate; PyBOP, benzotriazol-1-yloxytripyrrolidinophosphonium hexafluorophosphate.
- (29) (a) Wawzonek, S.; Gaffield, W. P., Jr. Synthesis of α -amino- β -(*p*-hydroxyphenoxy)propionamide hydrochloride. *Org. Prep. Proced. Int.* **1973**, *5*, 265–269. (b) Ager, D. J.; Fotheringham, I. G. Methods for the synthesis of unnatural amino acids. *Curr. Opin. Drug Discovery Dev.* **2001**, *4*, 800–807.
- (30) Evans, D. A.; Britton, T. C.; Dorow, R. L.; Dellaria, J. F., Jr. The asymmetric synthesis of α -amino and α -hydrazino acid derivatives via the stereoselective amination of chiral enolates with azodicarboxylate esters. *Tetrahedron* **1988**, *44*, 5525–5540.
- (31) Profft, E.; Becker, F. J. Condensation of β -aryl- β -amino acids with *o*-valero- and 6-caprolactim ethers, and cyclization of the condensation products. *J. Prakt. Chem.* **1965**, *30*, 18–38.
- (32) See the paragraph at the end of this paper regarding Supporting Information.
- (33) (a) Zasloff, M. Trypsin, for the defense. *Nat. Immunol.* **2002**, *3*, 508–510. (b) Ghosh, D.; Porter, E.; Shen, B.; Lee, S. K.; Wilk, D.; Drabza, J.; Yadav, S. P.; Crabb, J. W.; Ganz, T.; Bevins, C. L. Paneth cell trypsin is the processing enzyme for human defensin-5. *Nat. Immunol.* **2002**, *3*, 583–590. (c) Gumbmann, M. R.; Spangler, W. L.; Dugan, G. M.; Rackis, J. J. Safety of trypsin inhibitors in the diet: Effects on the rat pancreas of long-term feeding of soy flour and soy protein isolate. In *Nutritional and Toxicological Significance of Enzyme Inhibitors in Foods*; Friedman, M., Ed.; Plenum Press: New York, 1986; pp 33–79. (d) Gallaher, D.; Schneeman, B. O. Nutritional and metabolic response to plant inhibitors of digestive enzymes. In *Nutritional and Toxicological Significance of Enzyme Inhibitors in Foods*; Friedman, M., Ed.; Plenum Press: New York, 1986; pp 167–184. (e) Wilson, P. A.; Melmed, R. N.; Hampe, M. M. V.; Holt, S. J. Immunocytochemical study of the interaction of soybean trypsin inhibitor with rat intestinal mucosa. *Gut* **1978**, *19*, 260–266. (f) Grant, G. Anti-nutritional effects of soyabean: A review. *Prog. Food Nutr. Sci.* **1989**, *13*, 317–348.
- (34) However, it is worthwhile to note that melagatran, which potentially inhibits thrombin and trypsin (K_i values of 2 and 4 nM, respectively), and ximelagatran, its double prodrug form, have been well tolerated in human clinical trials: Sorbera, L. A.; Bayes, M.; Castaner, J.; Silvestre, J. Melagatran and ximelagatran: anticoagulant thrombin inhibitor. *Drugs Future* **2001**, *26*, 1155–1170. Gustafsson, D.; Nystrom, J.-E.; Carlsson, S.; Bredberg, U.; Eriksson, U.; Gyzander, E.; Elg, M.; Antonsson, T.; Hoffmann, K.-J.; Ungell, A.-L.; Sorensen, H.; Nagard, S.; Abrahamsson, A.; Bylund, R. The direct thrombin inhibitor melagatran and its oral prodrug H 376/95: Intestinal absorption properties, biochemical and pharmacodynamic effects. *Thromb. Res.* **2001**, *101*, 171–181. Sarich, T. C.; Eriksson, U. G.; Mattsson, C.; Wolzt, M.; Frison, L.; Fager, G.; Gustafsson, D. Inhibition of thrombin generation by the oral direct thrombin inhibitor ximelagatran in shed blood from healthy male subjects. *Thromb. Haemostasis* **2002**, *87*, 300–305. Hopfner, R. Ximelagatran (AstraZeneca). *Curr. Opin. Invest. Drugs* **2002**, *3*, 246–251.
- (35) Recacha, R.; Carson, M.; Costanzo, M. J.; Maryanoff, B.; DeLucas, L. J.; Chattopadhyay, D. Structure of the RWJ-51084-bovine pancreatic β -trypsin complex at 1.8 Å. *Acta Crystallogr.* **1999**, *D55*, 1785–1791.
- (36) Shuman, R. T.; Rothenberger, R. B.; Campbell, C. S.; Smith, G. F.; Gifford-Moore, D. S.; Paschal, J. W.; Gesellchen, P. D. Structure–activity study of tripeptide thrombin inhibitors using α -alkyl amino acids and other conformationally constrained amino acid substitutions. *J. Med. Chem.* **1995**, *38*, 4446–4453.
- (37) (a) Claeson, G.; Philipp, M.; Agner, E.; Scully, M. F.; Metternich, R.; Kakkar, V. V.; DeSoyza, T.; Niu, L. H. Benzylloxycarbonyl-D-Phe-Pro-methoxypropylboroglycine: A novel inhibitor of thrombin with high selectivity containing a neutral side chain at the P1 position. *Biochem. J.* **1993**, *290*, 309–312. (b) Deadman, J. J.; Elgendy, S.; Goodwin, C. A.; Green, D.; Baban, J. A.; Patel, G.; Skordalakes, E.; Chino, N.; Claeson, G.; Kakkar, V. V.; Scully, M. F. Characterization of a class of peptide boronates with neutral P1 side chains as highly selective inhibitors of thrombin. *J. Med. Chem.* **1995**, *38*, 1511–1522. (c) Claeson, G.; Cheng, L.; Chino, N.; Deadman, J.; Elgendy, S.; Kakkar, V. V.; Scully, M. F.; Philipp, M.; Lundin, R.; Mattson, C. Novel peptide mimetics as highly efficient inhibitors of thrombin based on modified D-Phe-Pro-Arg sequences. *Pept.: Chem., Struct. Biol., Proc. Am. Pept. Symp.* **1992**, 824–825.
- (38) (a) Chan, A. W. E.; Golec, J. M. C. Prediction of relative potency of ketone protease inhibitors using molecular orbital theory. *Bioorg. Med. Chem.* **1996**, *4*, 1673–1677. (b) Abbotto, A.; Bradamante, S.; Pagani, G. A. Diheteroarylmethanes. 5. *E–Z* Isomerism of carbanions substituted by 1,3-azoles: ¹³C and ¹⁵N π charge/shift relationships as a source for mapping charge and ranking the electron-withdrawing power of heterocycles. *J. Org. Chem.* **1996**, *61*, 1761–1769.
- (39) (a) Cutrona, K. J.; Sanderson, P. E. J. The synthesis of thrombin inhibitor L-370,518 via an α -hydroxy- β -lactam. *Tetrahedron Lett.* **1996**, *37*, 5045–5048. (b) Lyle, T. A.; Chen, Z.; Appleby, S. D.; Freidinger, R. M.; Gardell, S. J.; Lewis, S. D.; Li, Y.; Lyle, E. A.; Lynch, J. J., Jr.; Mulichak, A. M.; Ng, A. S.; Naylor-Olsen, A. M.; Sanders, W. M. Synthesis, evaluation, and crystallographic analysis of L-371,912: a potent and selective active-site thrombin inhibitor. *Bioorg. Med. Chem. Lett.* **1997**, *7*, 67–72.
- (40) Fevig, J. M.; Buriak, J., Jr.; Cacciola, J.; Alexander, R. S.; Kettner, C. A.; Knabb, R. M.; Pruitt, J. R.; Weber, P. C.; Wexler, R. R. Rational design of boropeptide thrombin inhibitors: β , β -dialkyl-phenethylglycine P2 analogs of DuP 714 with greater selectivity over complement factor 1 and an improved safety profile. *Bioorg. Med. Chem. Lett.* **1998**, *8*, 301–306.
- (41) (a) Levy, O. E.; Semple, J. E.; Lim, M. L.; Reiner, J.; Rote, W. E.; Dempsey, E.; Richard, B. M.; Zhang, E.; Tulinsky, A.; Ripka, W. C.; Nutt, R. F. Potent and selective thrombin inhibitors incorporating the constrained arginine mimic L-3-piperidyl(N-guanidino)alanine at P1. *J. Med. Chem.* **1996**, *39*, 4527–4530. (b) Semple, J. E.; Rowley, D. C.; Brunck, T. K.; Ha-Uong, T.; Minami, N. K.; Owens, T. D.; Tamura, S. Y.; Goldman, E. A.; Siev, D. V.; Ardecky, R. J.; Carpenter, S. H.; Ge, Y.; Richard, B.

- M.; Nolan, T. G.; Hakanson, K.; Tulinsky, A.; Nutt, R. F.; Ripka, W. C. Design, synthesis, and evolution of a novel, selective, and orally bioavailable class of thrombin inhibitors: P1-Argininal derivatives incorporating P3-P4 lactam sulfonamide moieties. *J. Med. Chem.* **1996**, *3*, 4531-4536. (c) Abelman, M. M.; Ardecky, R. J.; Nutt, R. F. Preparation of methionine sulfone and S-substituted cysteine sulfone derivatives as inhibitors of thrombin or factor Xa. PCT Int. Appl. WO 9528420, 1995.
- (42) Malley, M. F.; Taberero, L.; Chang, C. Y.; Ohringer, S. L.; Roberts, D. G. M.; Das, J.; Sack, J. S. Crystallographic determination of the structures of human α -thrombin complexed with BMS-186282 and BMS-189090. *Protein Sci.* **1996**, *5*, 221-228.
- (43) (a) Intravenous half-lives in rats were generally in the range of 15-40 min (e.g., **1b**, 22 min; **3**, 19 min; **4**, 25 min; **8**, 14 min; **14**, 26 min; **16**, 42 min; **68**, 43 min). (b) Intravenous infusion of **3** at doses of 3, 10, and 30 mg/kg in anesthetized guinea pigs was performed over 5 min, and the ECG was monitored. Compound **3** at the 3 mg/kg dose did not alter the ECG pattern. However, a 10 mg/kg dose of **3** resulted in a decrease in the amplitude of the R wave of the ECG. The T and P waves tended to merge during the time of peak response, at the end of infusion, and at 5 min after infusion. A 30 mg/kg dose of **3** resulted in an inversion of the QRS complex with a dramatic increase in the amplitude of the T wave immediately on completion of the infusion. The ECG continued to deteriorate at 5 min after infusion to a waveform similar to coarse fibrillation but yet rhythmic. At 20 and 60 min after infusion, the waveform reverted to an inverted QRS waveform with a T wave of increased amplitude.
- (44) Kaiser, B.; Hauptmann, J. Pharmacology of synthetic thrombin inhibitors of the tripeptide type. *Cardiovasc. Drug Rev.* **1992**, *10*, 71-87.
- (45) (a) In contrast to compound **3** (cf. ref 43b), intravenous infusion of **4** in anesthetized guinea pigs exhibited no effects on the ECG at the 3 and 10 mg/kg doses and only minor effects at the 30 mg/kg dose, including a tendency for the T and P waves to merge and a slight ST-segment deviation. These effects were observed for only a short period of time at the end of the infusion period, after which the waveform returned to normal. (b) Interestingly, a carboxylic acid moiety was used in the argatroban series to alleviate toxic effects. Okamoto, S.; Hijikata-Okunomiya, A.; Wanaka, K.; Okada, Y.; Okamoto, U. Enzyme-controlling medicines: introduction. *Semin. Thromb. Hemostasis* **1997**, *23*, 493-501. Kikumoto, R.; Tamao, Y.; Tezuka, T. Selective inhibition of thrombin by (2*R*,4*R*)-methyl-1-[N²-(3-methyl-1,2,3,4-tetrahydro-8-quinolinyl)sulfonyl]-L-arginyl]-2-piperidine-carboxylic acid. *Biochemistry* **1984**, *23*, 85-90.
- (46) Rees, D. D.; Palmer, R. M. J.; Schulz, R.; Hodson, H. F.; Moncada, S. Characterization of three inhibitors of endothelial nitric oxide synthase in vitro and in vivo. *Br. J. Pharmacol.* **1990**, *101*, 746-752.
- (47) Bellou, A.; Lambert, H.; Gillois, P.; Montemont, C.; Gerard, P.; Vauthier, E.; Sainte-Laudy, J.; Longrois, D.; Gueant, J. L.; Mallie, J. P. Constitutive nitric oxide synthase inhibition combined with histamine and serotonin receptor blockade improves the initial ovalbumin-induced arterial hypertension but decreases the survival time in brown Norway rats anaphylactic shock. *Shock* **2003**, *19*, 71-78.
- (48) Dunbar, J. C.; O'Leary, D. S.; Wang, G.; Wright-Richey, J. Mechanisms mediating insulin-induced hypotension in rats. A role for nitric oxide and autonomic mediators. *Acta Diabetol.* **1996**, *33*, 263-268.
- (49) Hoste, S.; Van Aken, H.; Stevens, E. Tranexamic acid in the treatment of anaphylactic shock. *Acta Anaesthesiol. Belg.* **1991**, *42*, 113-116.
- (50) Singer, L.; Colten, H. R.; Westel, R. A. Complement C3 deficiency: human, animal, and experimental models. *Pathobiology* **1994**, *62*, 14-28.
- (51) Skrzypczak-Jankun, E.; Carperos, J. E.; Ravichandran, K. G.; Tulinsky, A.; Westbrook, M.; Maraganore, J. M. Structure of the hirugen and hirulog 1 complexes of thrombin. *J. Mol. Biol.* **1991**, *221*, 1379-1393.
- (52) Wu, Q.; Sheehan, J. P.; Tsiang, M.; Lentz, R. S.; Birktoft, J. J.; Sadler, J. E. Single amino acid substitutions dissociate fibrinogen-clotting and thrombomodulin-binding activities of human thrombin. *Proc. Natl. Acad. Sci. U.S.A.* **1991**, *88*, 6775-6779.
- (53) (a) Qui, X.; Padmanabhan, K. P.; Carperos, V. E.; Tulinsky, A.; Kline, T.; Maraganore, J. M.; Fenton, J. W., II. Structure of the hirulog 3-thrombin complex and nature of the S' subsites of substrates and inhibitors. *Biochemistry* **1992**, *31*, 11689-11697. (b) Krishnan, R.; Tulinsky, A.; Vlasuk, G. P.; Pearson, D.; Vallar, P.; Bergum, P.; Brunck, T. K.; Ripka, W. C. Synthesis, structure and structure-activity relationships of divalent thrombin inhibitors containing an α -keto amide transition state mimetic. *Protein Sci.* **1996**, *5*, 422-433. (c) Mathews, I. I.; Tulinsky, A. Active site mimetic inhibition of thrombin. *Acta Crystallogr.* **1995**, *D51*, 550-559. (d) Tulinsky, A.; Qiu, X. Active Site and Exosite Binding of α -Thrombin. *Blood Coagulation Fibrinolysis* **1993**, *4*, 305-312. (e) Tulinsky, A. Molecular interactions of thrombin. *Semin. Thromb. Hemostasis* **1996**, *22*, 117-124.
- (54) (a) Goodford, P. J. A computational procedure for determining energetically favorable binding sites on biologically important molecules. *J. Med. Chem.* **1985**, *28*, 849-857. (b) Reynolds, C. A.; Wade, R. C.; Goodford, P. J. Identifying targets for bioreductive agents: using GRID to predict selective binding regions of proteins. *J. Mol. Graphics* **1989**, *7*, 103-108. (c) We used GRID, version 15; Molecular Discovery Ltd., West Way House, Elms Parade, Oxford OX2 9LL, U.K.
- (55) Please note that **3** was never considered for advancement into development because of its ECG and hypotensive side effects, contrary to a statement in a recent review article: Jorgensen, W. L. The many roles of computation in drug discovery. *Science* **2004**, *303*, 1813-1818. Similarly, **4** and **68** were not moved forward into preclinical development because of their poor pharmacokinetic properties.
- (56) Kiljunen, H.; Hase, T. A. Titration of organolithiums and Grignards with 1-pyreneacetic acid. *J. Org. Chem.* **1991**, *56*, 6950-6952.
- (57) Turk, J.; Panse, G. T.; Marshall, G. R. α -Methyl amino acids. Resolution and amino protection. *J. Org. Chem.* **1975**, *40*, 953-955.
- (58) Kwon, C. H.; Iqbal, M. T.; Wurlpel, J. N. D. Synthesis and anticonvulsant activity of 2-iminohydantoins. *J. Med. Chem.* **1991**, *34*, 1845-1849.
- (59) For the synthesis of Boc-L-Arg(Mtr)N(OMe)Me, see the following: Deng, J.; Hamada, Y.; Shioiri, T.; Matsunaga, S.; Fusetani, N. Synthesis of cyclotheonamide B and derivatives. *Angew. Chem., Int. Ed. Engl.* **1994**, *33*, 1729-1731. Kahn, M. PCT Int. Appl. WO9630396 A1, 1996 (example 2).
- (60) Kent, D. R.; Cody, W. L.; Doherty, A. M. The asymmetric synthesis of arginine mimetics: derivatives of (S)-2-, 3- and 4-amidinophenylalanine suitable for incorporation into enzyme inhibitors and/or peptides. *J. Pept. Res.* **1998**, *52*, 201-207.
- (61) (a) Wagner, G.; Richter, P.; Garbe, C. Syntheses of 3-[amidinophenyl]alanines and 3-[amidinophenyl]lactic acids. *Pharmazie* **1974**, *29*, 12-15. (b) Levy, O. E.; Tamura, S. Y.; Nutt, R. F.; Ripka, W. C. Preparation of peptide aldehyde derivatives as arginine mimics and enzyme thrombin inhibitors. PCT Int. Appl. WO 9535312, 1995.
- (62) Kirmse, W.; Jansen, U. Deamination reactions. 41. Reactions of aliphatic diazonium ions and carbocations with ethers. *Chem. Ber.* **1985**, *118*, 2607-2625.
- (63) Evans, D. A.; Britton, T. C.; Dellaria, J. F. The asymmetric synthesis of α -amino and α -hydrazino acid derivatives via the stereoselective amination of chiral enolates with azodicarboxylate esters. *Tetrahedron* **1988**, *44*, 5525-5540.
- (64) Ellingboe, J. W.; Spinelli, W.; Winkley, M. W.; Nguyen, T. T.; Parsons, R. W.; Moubarak, I. F.; Kitzen, J. M.; Von Engen, D.; Bagli, J. F. Class III antiarrhythmic activity of novel substituted 4-[(methylsulfonyl)amino]benzamides and sulfonamides. *J. Med. Chem.* **1992**, *35*, 705-16.
- (65) Guichard, G.; Briand, J. P.; Friede, M. Synthesis of arginine aldehydes for the preparation of pseudopeptides. *Peptide Res.* **1993**, *6*, 121-124.
- (66) Ambrogi, V.; Grandolini, G.; Perioli, L.; Rossi, C. Convenient synthesis of 2-aminonaphthalene-1-thiol and 3-aminoquinoline-4-thiol and cyclocondensations to 1,4-thiazino and 1,4-thiazepino derivatives. *Synthesis* **1992**, *7*, 656-658.
- (67) Friedman, M. D.; Stotter, P. L.; Porter, T. H.; Folkers, K. Coenzyme Q. 166. Antimetabolites of coenzyme Q. 21. Synthesis of alkyl-4,7-dioxobenzothiazoles with prophylactic antimalarial activity. *J. Med. Chem.* **1973**, *16*, 1314-1316.
- (68) Huang, W.; Naughton, M. A.; Yang, H.; Su, T.; Dam, S.; Wong, P. W.; Arfsten, A.; Edwards, S.; Sinha, U.; Hollenbach, S.; Scarborough, R. M.; Zhu, B.-Y. Design, synthesis, and structure-activity relationships of unsubstituted piperazinone-based transition state factor Xa inhibitors. *Bioorg. Med. Chem. Lett.* **2003**, *13*, 723-728.
- (69) Hakansson, K.; Tulinsky, A.; Abelman, M. M.; Miller, T. A.; Vlasuk, G. P.; Bergum, P. W.; Lim-Wilby, M. S. L.; Brunck, T. K. Crystallographic structure of a peptidyl keto acid inhibitor and human α -thrombin. *Bioorg. Med. Chem.* **1995**, *3*, 1009-1017.
- (70) (a) Williams, J. W.; Morrison, J. F. The kinetics of reversible tight-binding inhibition. *Methods Enzymol.* **1979**, *63*, 437-467. (b) Morrison, J. F. The slow-binding and slow, tight-binding inhibition of enzyme-catalyzed reactions. *Trends Biochem. Sci.* **1982**, *7*, 102-105.